Bendix

Aerospace Systems Division

HFE BIREFLECTOR THERMAL DESIGN AND TEST RESULTS

NO. ATM 895	REV. NO.
PAGE 1 OF 63	
DATE 6/29/70	

This ATM summarizes the analytical and test results of the nominal ALSEP bireflector HFE electronics package assembly thermal control system which was developed for use at the lunar equator. The test results summarized include the engineering component and ALSEP system thermal/vacuum tests. The analytical effort includes the thermal performance of the electronics package assembly at off-equator deployment sites up to 60° latitude which was conducted as a part of the direction received under Bendix CCP 216.

Prepared by: J. A. Griffin, Jr.
J. Griffin

Prepared by: D. Psaros
G. Psaros

Approved by: J. McNaughton
J. McNaughton

CONTENTS

CONTENTS (CONT.)

ILLUSTRATIONS

TABLES

1.0 INTRODUCTION

The Heat Flow Experiment (HFE) is designed to measure the lunar temperature gradients and soil thermal conductivity from the surface to depths of ten feet. The experiment consists of two sensor probes and the Electronics Package Assembly (EPA) as shown in Figure 1.1. The EPA thermal control system is required to maintain the electronic components between temperatures of 32 and 140°F (0 to 60°C) during an entire lunation to achieve desirable experiment accuracy. This study is concerned exclusively with the thermal control of the electronics package assembly.

The original specifications called for the HFE to be deployed at landing sites within ±5 degrees from the equator. A thermal control system to operate within this deployment constraint was designed. Thermal control of the EPA was achieved by using the following design techniques:

1. Attaching the electronics to a horizontal aluminum thermal plate.

2. Providing a sunshield to protect the thermal plate from direct solar impingement when aligned within the equatorial plane.

3. Using two specular reflectors to provide the thermal radiator plate with a better view to space and to minimize the view of the lunar surface.

4. Thermally insulating the electronic housing with multilayer aluminized mylar.

5. Applying a low solar absorptance/infrared emittance thermal control coating to all external surfaces except reflectors.

6. Providing heater power to maintain desired temperatures during lunar night.

7. Attaching a multilayer insulation mask to the thermal plate to provide the required temperature swing and to prevent direct solar impingement due to EPA leveling errors, east-west misalignment and the possible ±5 degrees deployment latitude from the equator.

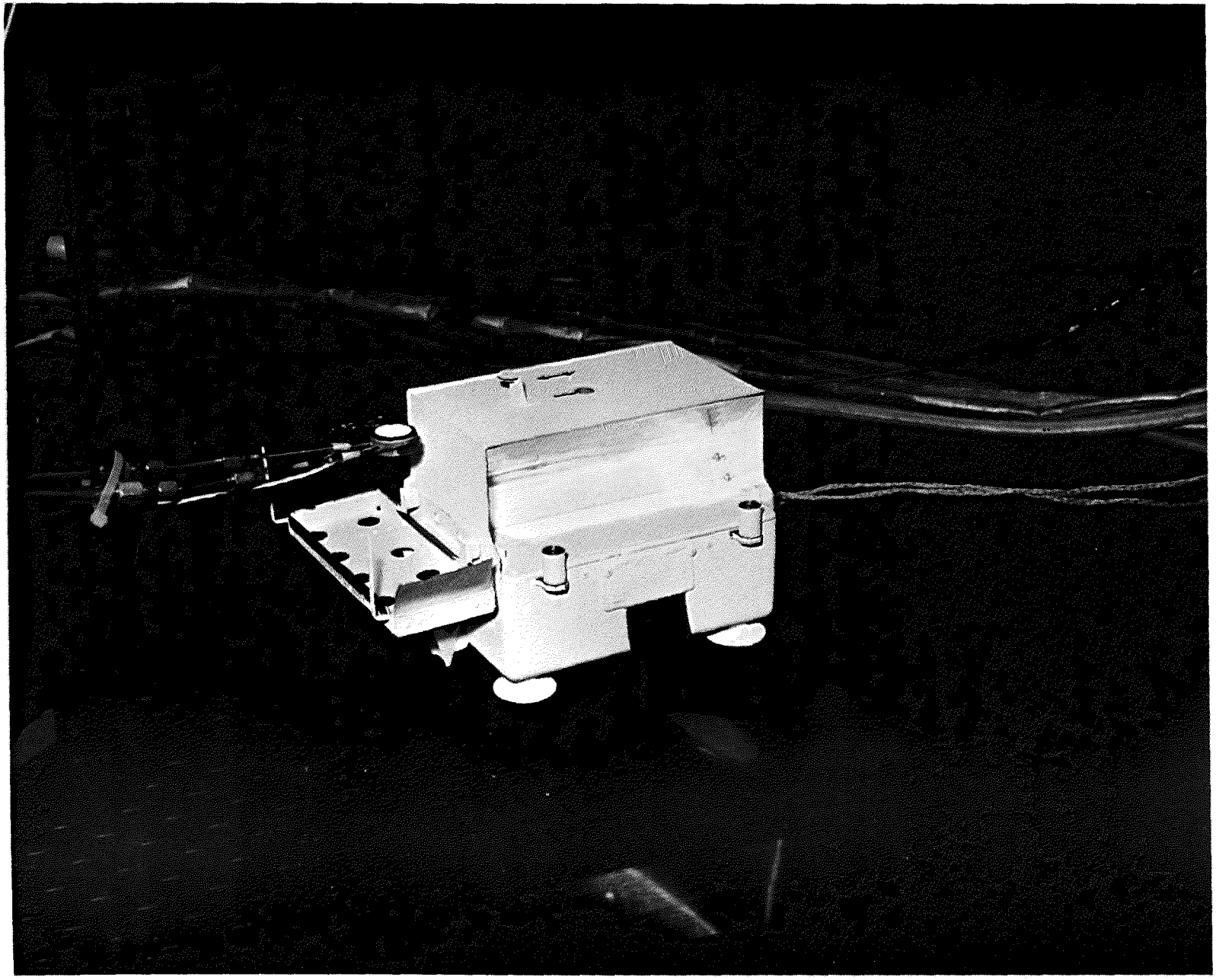

Figure 1.1 Bireflector HFE Electronics Package Assembly

The development of the thermal control system for the HFE electronics package assembly (EPA) included (1) a detailed analytical study to establish the pertinent parameters (ref. 2), (2) an engineering thermal/vacuum test (ETV) of a thermal model to verify the conceptual design, (3) a design verification thermal/vacuum test (DVTV) to verify the actual hardware, (4) a qualification acceptance thermal/vacuum test (QATV) to qualify the hardware at qualification temperature levels and heat loads, and (5) a flight acceptance thermal/vacuum test (FATV) for customer approval.

Reference 9 summarizes the parametric studies and analyses of the HFE EPA thermal control system. The thermal analysis includes a parametric study of a 4, 6 and 8-inch wide by 10-inch long sunshield. Up to this study, an 8-inch wide sunshield was the nominal configuration since the metal heat sink plate (i.e. the radiator plate), to which the electronics were bolted, was 8 inches wide by 10 inches long. Thus, the sunshield originally covered the entire metal heat sink plate. The parametric study in ref. 9 revealed that the narrower the sunshield, the better the temperature control of the radiator plate. The misalignment capability of the HFE EPA decreased with decreasing width. It was then concluded that the 6-inch wide sunshield would result in the lowest temperature excursion of the three widths studied when considering the deployment process on the moon (i.e. the distance of the landing site from the lunar equator or subsolar path, the slope of the lunar terrain, and the leveling capabilities of the EPA by the astronaut).

The BxA ALSEP thermal/vacuum testing series began when the nominal sunshield width was 8 inches. This ETV test was performed at the Beech Aircraft facilities at Boulder, Colorado. When the decision to mount the 6-inch wide sunshield was made, the HFE EPA thermal model was again ETV tested; this time at the MSC (SEEL) facilities. These tests did verify the validity of the 6-inch wide sunshield design concept and thermal analysis. The actual hardware was then tested in the BxA 20' x 25' thermal/vacuum chamber. The HFE DVTV was conducted to verify the functioning of the actual hardware; the QATV-SB to further qualify the hardware; and the FATV-3 for customer approval.

However, currently proposed lunar landing sites now call for the HFE to be deployed at latitudes other than those for which it was originally designed. Future non-equatorial deployments at latitudes of up to 45° may find the present symmetrical EPA thermal control system inadequate.

To determine the effects of the off-equatorial deployment, an updated analytical thermal model of the electronics package was developed and correlated with test results. Thermal plate temperature of the present design is determined as a function of the deployment latitude and degradation of surface properties by dust coverage. The existance of potential material problems due to dust coverage and direct solar impingement of the reflector and specular side curtains were investigated.

This report documents the analytical model and presents temperature predictions for both day and night.

2.0 SUMMARY OF RESULTS

The HFE EPA bireflector thermal control system is adequate to maintain the thermal radiator plate (i.e. the electronics metal heat sink) within the required specification of 0°C to 60°C (i.e. 32°F to 140°F) with the experiment in nominal operation at the lunar equator and with any external environment from (A) the nominal ALSEP environment of 1 solar constant and lunar surface extremes from 250. ± 10.0°F to -300. ±20.0 °F to (B) the ALSEP design limit condition of 1.25 solar constants and lunar surface extremes from 280.0 ± 10°F to -300.0 ± 20°F. The thermal radiator plate will also be maintained within its required operating temperature limits at the lunar equator for totally degraded surfaces that are exposed to solar radiation.

Results of the BxA ALSEP series of thermal/vacuum tests have been summarized for the HFE electronics package assembly (EPA) thermal control system. A table is presented that summarizes the general test conditions and HFE EPA configurations of each test. The lunar surface simulation for each test is compared relative to the actual lunar surface. The thermal radiator plate temperatures and the lunar noon-night temperature excursions are summarized in tables for the conditions tested. For the HFE EPA models possessing the HK temperature sensor, the temperatures indicated are compared with the available thermocouple data. A

graphical presentation of the thermal radiator plate temperatures at the lunar noon and night conditions are shown as a function of internal power dissipation. This is necessary for a direct comparison between models and thermal/vacuum tests since internal power differs between models.

The results of these tests show that the original lower operating limit of 50°F (i.e. 10°C) of reference 25 was exceeded in thermal/vacuum tests where the actual hardware was tested. This operating limit has been revised to 32°F (i.e. 0°C) in reference 25 since the electronics were found to operate accurately at the temperatures that the electronics experienced during the thermal/vacuum testing.

The specified lunar noon - night temperature excursion of 90°F (i.e. 50°C) was exceeded in the design verification and the Qual SB acceptance thermal/vacuum tests (i.e. DVTV and QATV-SB). This was due primarily to the conditions imposed on the HFE EPA in these tests; the test conditions being more severe than the expected conditions on the lunar surface. The QATV-SB lunar surface simulator moderately over-simulated a flat infinite lunar surface. However, this condition could be realized if the HFE EPA is deployed in a lunar depression or in the vicinity of lunar rocks and/or geological formations of higher elevation. In the Flight #3 acceptance thermal/vacuum test (FATV-3) with the nominal lunar noon conditions imposed on the HFE EPA, the thermal radiator plate was maintained well within the specified temperature excursion.

Also, presented is a table of items that could affect the HFE EPA thermal control system. This table is presented in the event that a lesser temperature excursion is desired for the thermal radiator plate.

The thermal performance of the bireflector heat flow electronics package assembly has been determined for deployment sites ranging from the equator to ±60° latitude. In general for thermal control surfaces which retain their nominal optical properties and are not dust degraded, the thermal plate temperature remains below the maximum specified temperature of 140°F. However, if the surfaces are moderately dust degraded, the thermal

plate temperatures exceed the specified limit at a latitude of 19 degrees. For heavy dust covered surfaces, it is impossible to maintain desired thermal control of the package except for deployment sites near the equator. With certain combinations of degradation and deployment latitude, the maximum specified temperature is exceeded by more than 100 °F.

Therefore, the thermal control system of the EPA must be modified if it is to be deployed at latitudes other than the equator.

3.0 DESIGN REQUIREMENTS AND CONSTRAINTS

3.0.1 ALSEP Requirements (ref. 23)

1 High Reliability - Passive Thermal Control Design with Electrical Heaters

2 Landing Site ± 5° from Lunar Equator

3 All surfaces of the EPA exposed to direct solar radiation are fully degraded. (i.e. $\alpha_S/\epsilon_{IR} = 0.9/0.9$) due to:

1. Vacuum radiation effects
2. Lunar dust particles.

3.0.2 Experiment Requirements (ref. 24)

1 Maintain radiator plate within 60°C (i.e. 108°F) temperature range in operating modes with total power available at night of 9.3 watts.

2 Maintain radiator plate within -50 to 70°C (i.e. -58 to 158°F) temperature range in survival mode with 3.8 watts of available power.

3 Level EPA to ± 12° from vertical.

4 Aligh EPA to ± 5° from the East-west line of sight.

3.1 HFE DESIGN ANALYSIS

A 32 node analytical model was developed to thermally simulate the HFE as deployed in the thermal vacuum chamber configuration and on the lunar surface. Both lunar noon and night steady state analyses were made. The effect of dust degradation was investigated by increasing the solar absorptance from the nominal value of α_s = 0.2 to 0.6 and 0.9. Lunar sunrise steady state temperatures were also determined. The sensitivity of the thermal plate temperature to varying amounts of electronic power dissipation was also studied.

3.2 ANALYTICAL RESULTS

3.2.1 Lunar Noon

The average thermal plate temperature at lunar noon as a function of latitude is presented in Figure 3.1 for both nominal and degraded surface conditions assuming the nominal power dissipation of 3.8 watts in mode I. Performance of the system with surfaces having nominal surface properties is acceptable for all latitudes of deployment. A maximum thermal plate temperature of 123.5°F occuring at 45° latitude is considerably below the specified maximum temperature of 140°F.

For the case of a moderate amount of dust coverage (α_s = 0.6), the thermal plate temperature increases from 120°F at the equator to 188°F at 45° latitude. For complete dust coverage (α_s = 0.9) the equatorial steady state temperature is 138°F. A maximum temperature of 218°F occurs at 45 degrees latitude.

These relatively high temperatures are a result of the direct solar impingement on the thermal plate and reflector surface. The effectiveness of the sunshield in shielding the radiator is reduced since at high latitudes one half of the thermal plate and the corresponding reflector is directly illuminated. The reflector temperature as a function of latitude is presented in Figure 3.2 for a nominal solar absorpance of 0.20. For deployment latitudes greater than 42.5 degrees the material temperature limit of 300°F was exceeded.

Figure 3.1 Thermal Plate Temperature at Lunar Noon vs. Latitude and Dust Degradation

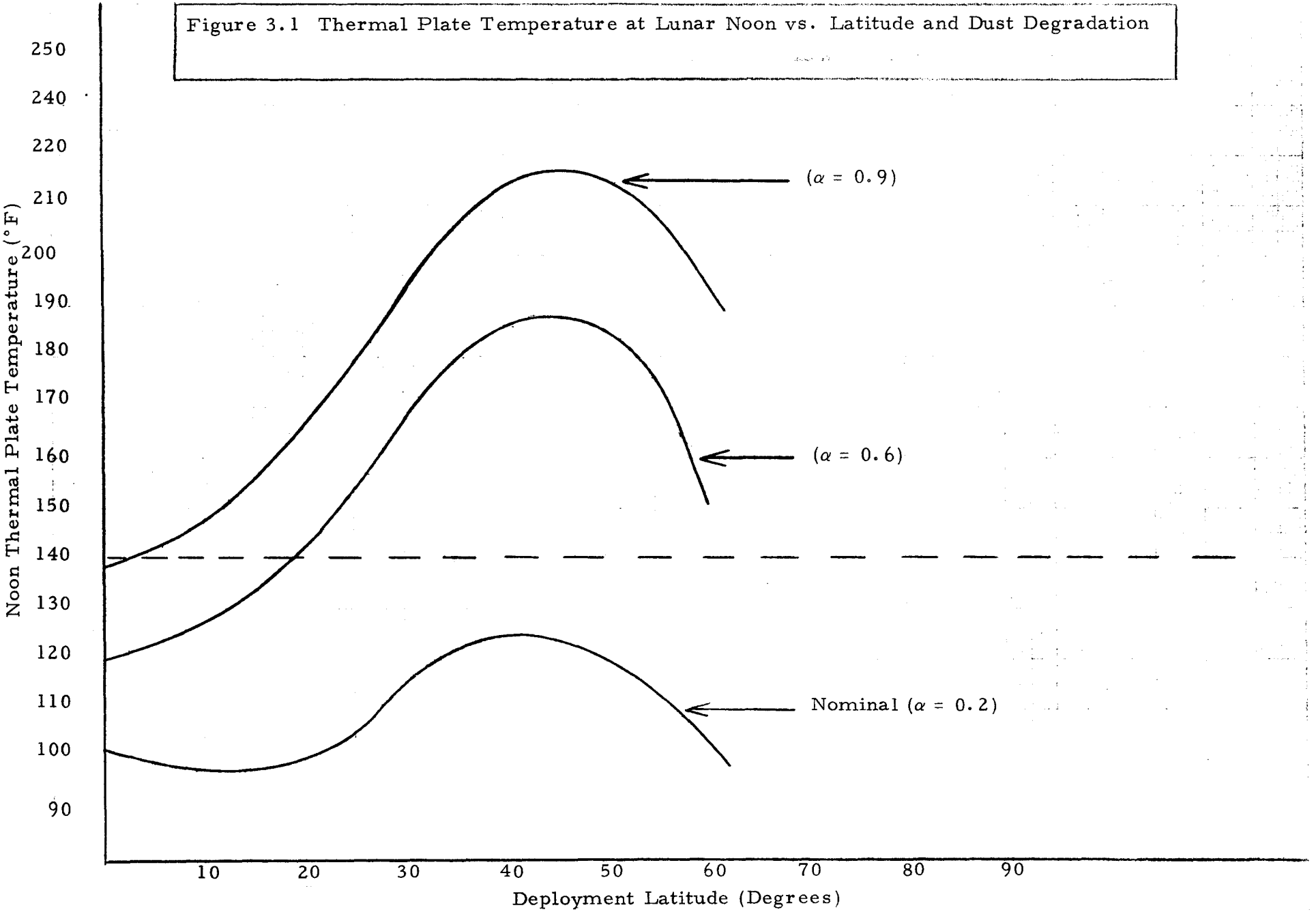

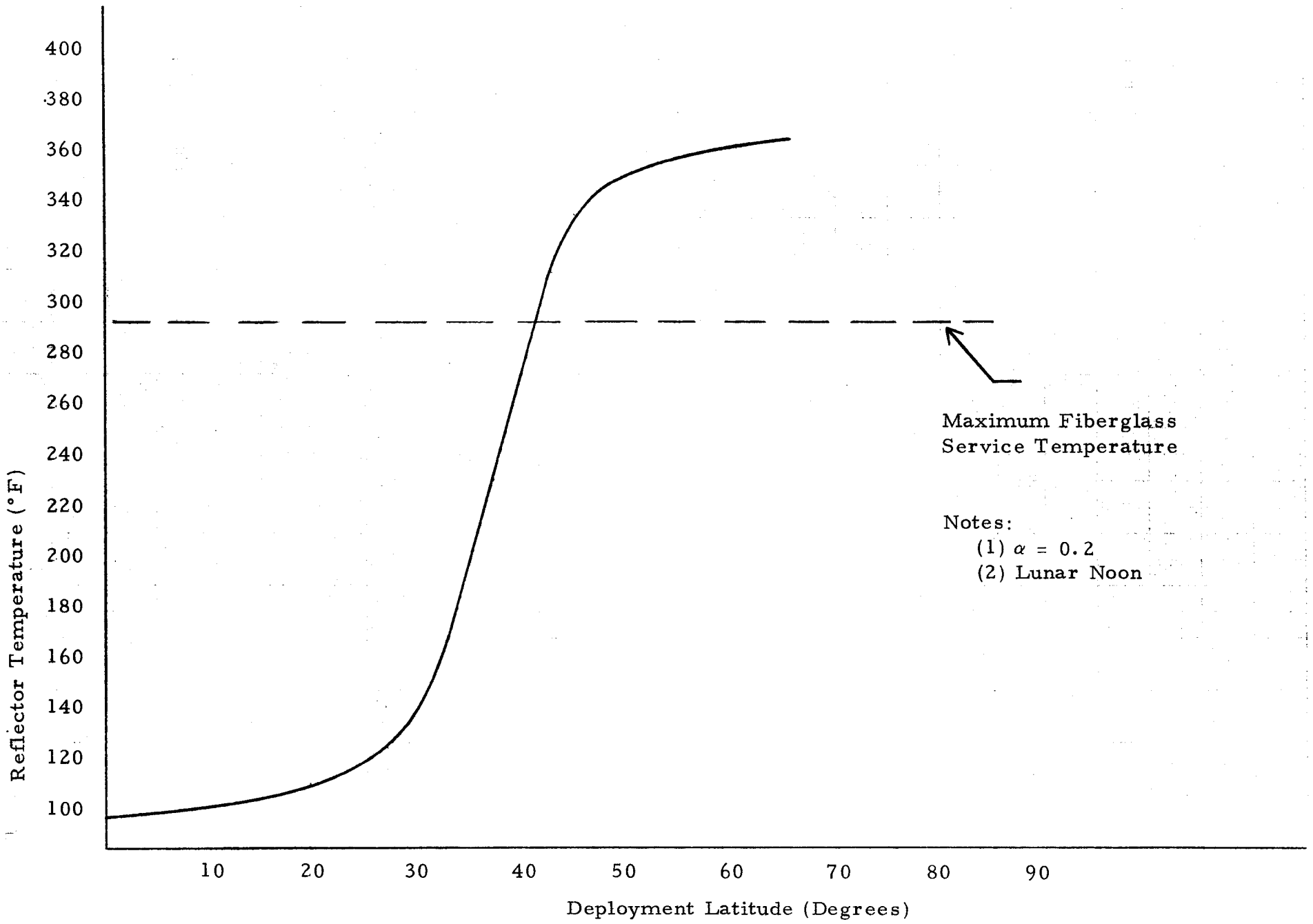

Fig. 3.2 Reflector Temperature vs. Deployment Latitude at Lunar Noon

Degraded surfaces due to Lunar Module ascent should be assumed. It is immediately evident from these results that the present electronics package thermal control system is inadequate for off-equatorial deployment.

3.2.2 Lunar Sunrise

Lunar sunrise conditions were considered since in general for non-equatorial deployment of the HFE the side curtains will be directly illuminated. Presented in Figure 3.3 are the temperatures of the side curtains and the reflector for nominal surface properties, α_s/ϵ_{ir} = 0.2/0.05. Steady state temperatures are shown for lunar surface temperatures of +250 and -300°F. Since the -300°F lunar surface temperatures more closely approximates conditions at lunar sunrise, no material failure should occur.

3.2.3 Lunar Night

With a lunar surface temperature of -300°F and the nominal internal electronics power dissipation of 9.3 watts, the thermal plate temperature is 45.7°F.

3.2.4 Effect of Electronic Power Dissipation on Average Thermal Plate Temperatures

Earlier parametric studies (reference 2) of thermal plate temperatures vs. internal power dissipation were made. Shown in Figure 3.4 is the thermal plate temperature of the updated model as a function of internal power dissipation for the lunar night. These temperatures are valid regardless of the deployment latitude. Also presented is the thermal plate temperature as a function of internal power dissipation at lunar noon for an equatorial deployment assuming nominal surface properties. The variation of steady state temperatures with power for lunar noon and night conditions are 10.8°F/watt and 17.6°F/watt, respectively.

3.3 DESCRIPTION OF THE ANALYTICAL MODEL

3.3.1 Node Description

The thermal model consists of 30 nodes representing components of the EPA. Two nodes representing the lunar surface and space are

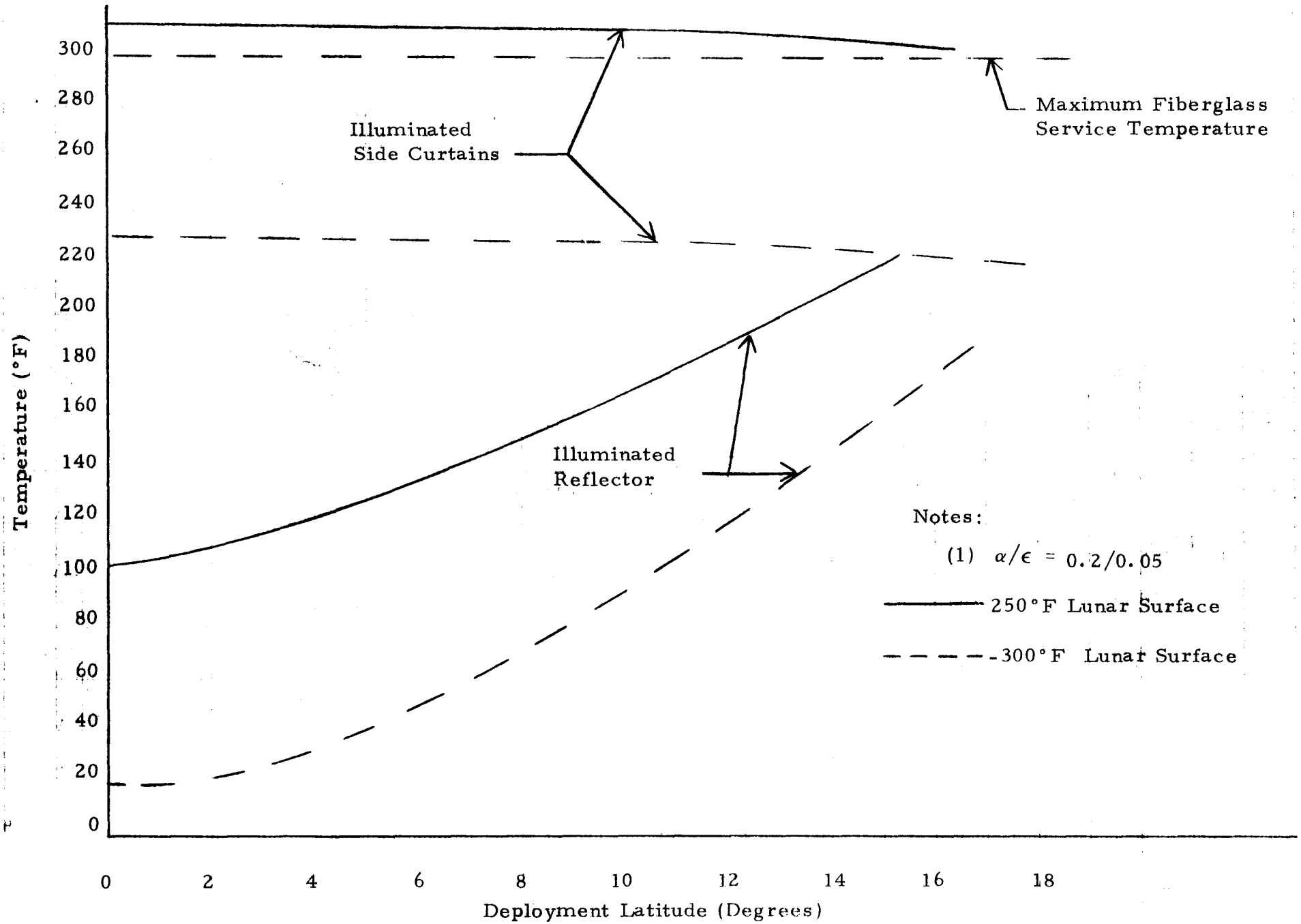

Figure 3.3 Lunar Sunrise Temperatures

Figure 3.4 Electronic Power Dissipation vs. Thermal Plate Temperature

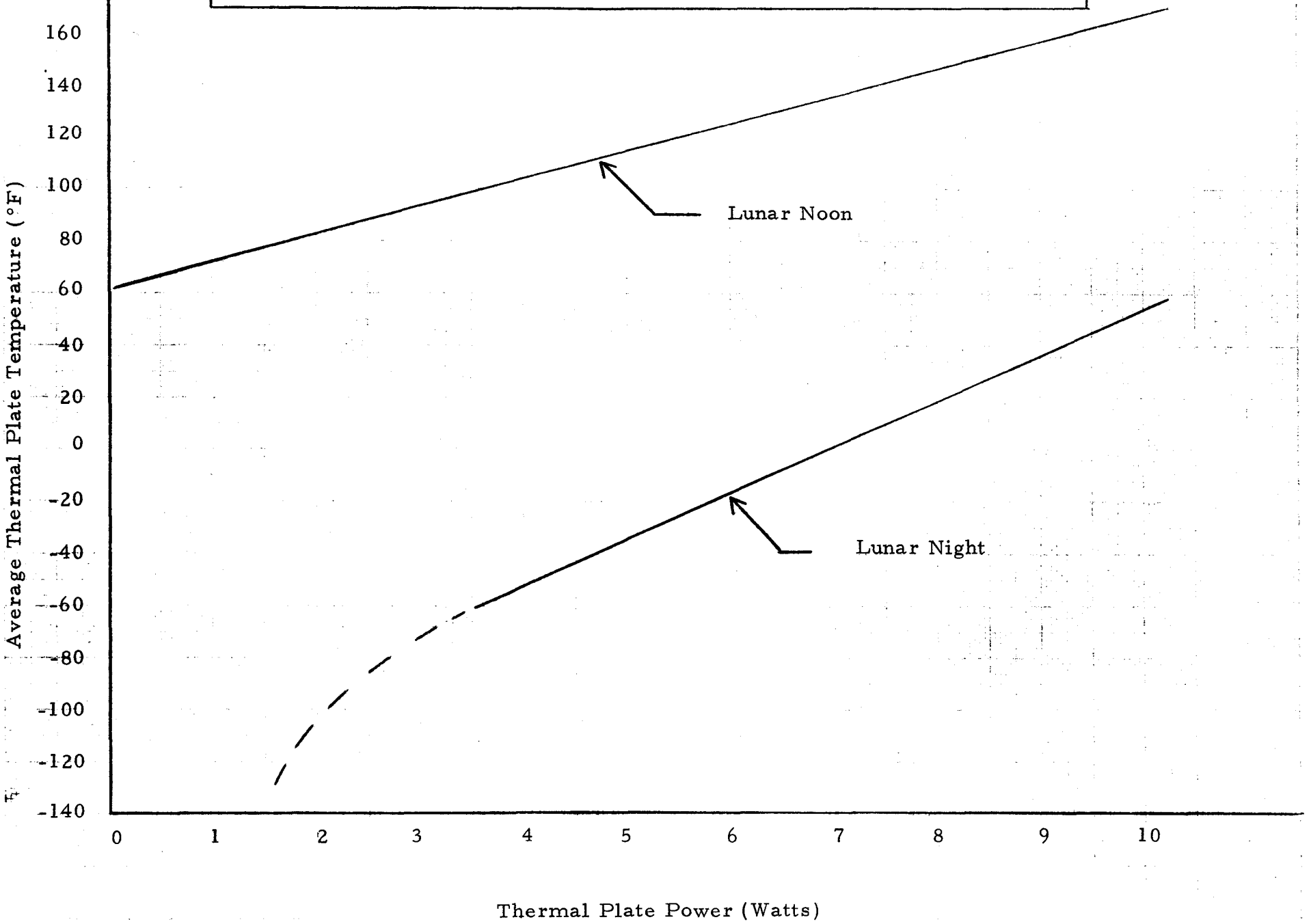

maintained at constant temperature. Figures 3.5 and 3.6 indicate the nodal locations. Table 3.1 lists the nodes, their physical description and pertinent thermal parameter values. The steady-state temperatures were determined using the Bendix Thermal Analyzer Computer Program.

3.3.2 Radiation Resistor Network

The values of the resistors for the radiation resistance network were obtained in several ways. For the partial enclosure formed by the side curtains, radiator plate, and reflector, the values of the resistances, were obtained using the radiosity method to account for multiple reflections. It was assumed that the specular surfaces of the side curtains could be treated as diffuse surfaces in order to simplify the problem of numerous multiple images that are necessary if those surfaces were treated as specular reflectors. The values of the resistances between the thermal bag and the thermal plate nodes were obtained by using values of configuration factors obtained through the use of configuration factor tables. The enclosure formed by the top, the two sides and the specular reflectors was also analyzed by this method. The values of the resistors are listed in Appendix 1.

3.3.3 Conduction Resistor Network

The effects of conduction heat transfer between the four segments of the thermal plate and the supporting framework were considered. Provisions were made for conduction through and between the various segments of the thermal bag. In addition, conduction paths were set up through the legs to the lunar surface.

Each resistor was initially determined analytically based on material dimensions as indicated on the existing drawings and a nominal value of thermal conductivity. These values were then adjusted in a number of cases to produce an average thermal plate temperature compariable to that obtained in the full scale thermal vacuum tests. These alterations were required to account for the variation in the thermal conductivity with temperature and the actual dimensions of the hardware as compared to the specified values. Appendix 3 lists the values of the conduction resistors.

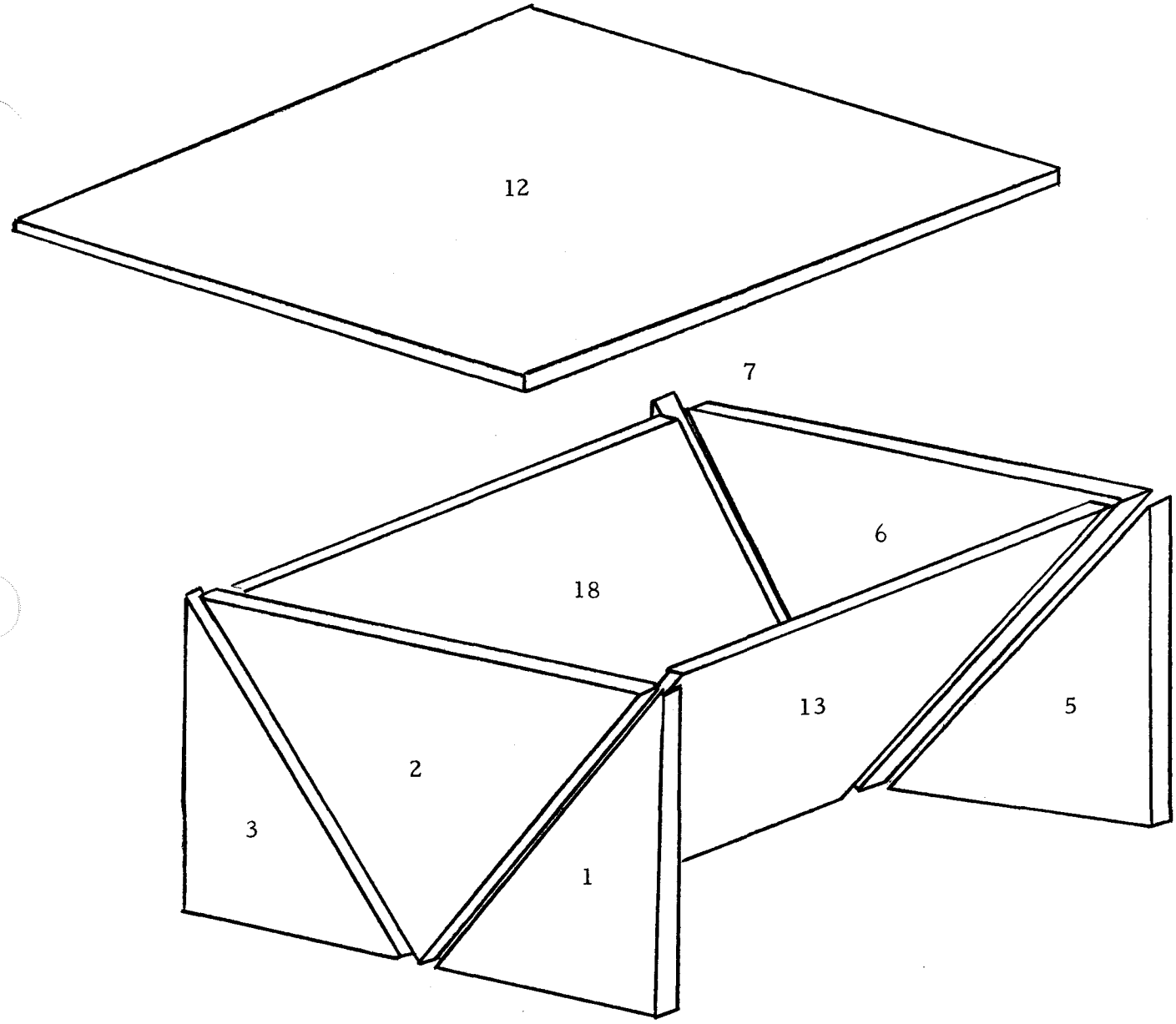

Figure 3.5 Reflector and Sunshield Nodes

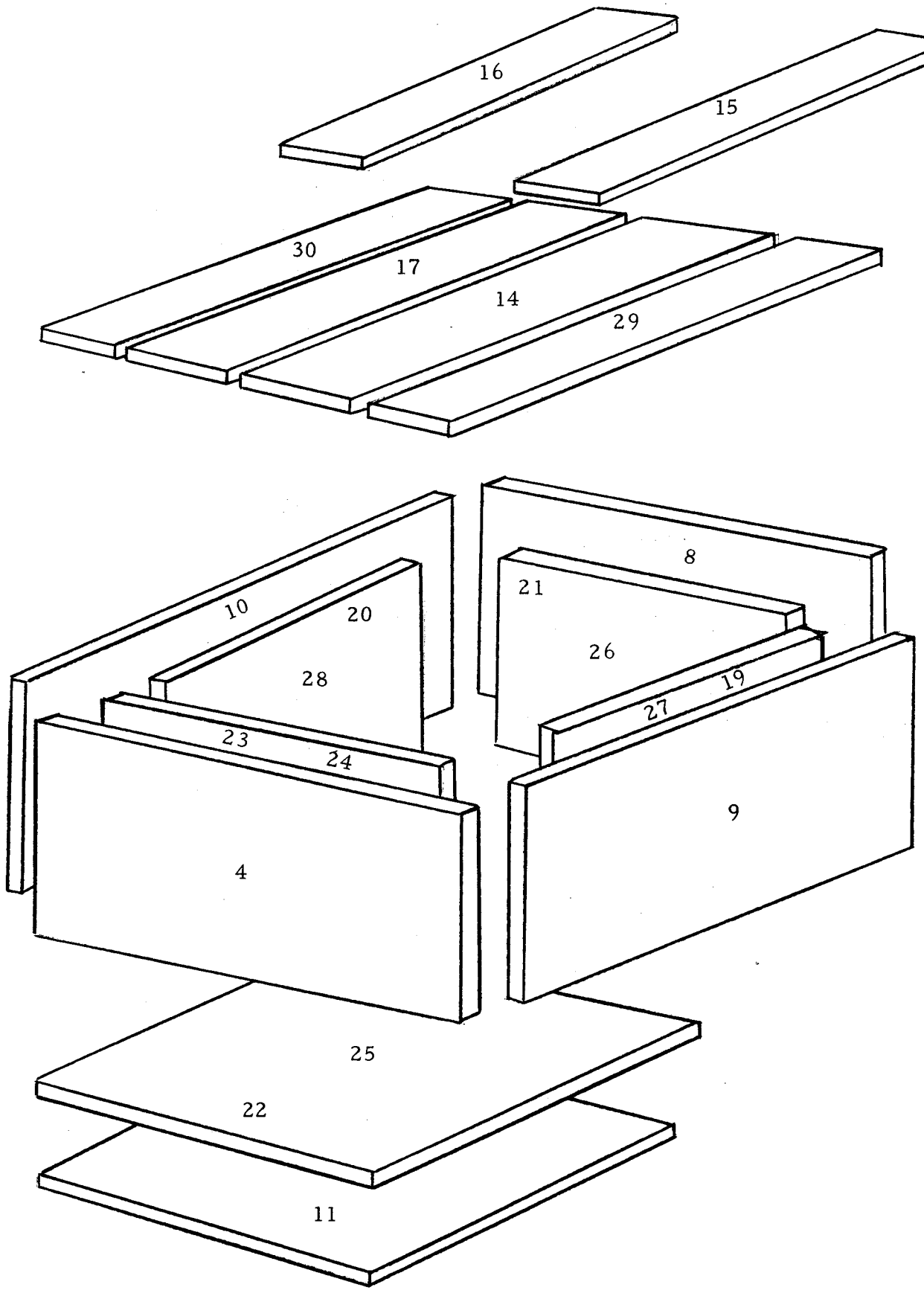

Figure 3.6 Thermal Plate, Bag and Enclosure Nodes

TABLE 3.1

NODE PROPERTIES AND PHYSICAL DESCRIPTION

Node No.	Corresponding Radiosity Node	Description	Area (ft^2)	Emissivity	Conductivity $\frac{(Btu/hr)}{ft\,°F}$
1	101	Side Curtain	.041667	.05	.2
2	102	Side Triangle	.083	.9	.2
3	103	Side Curtain	.041667	.05	.2
4	104	Side	.192	.9	.2
5	105	Side Curtain	.041667	.05	.2
6	106	Side Triangle	.083	.9	.2
7	107	Side Curtain	.041667	.05	.2
8	108	Side	.192	.9	.2
9	109	Front	.241	.9	.2
10	110	Rear	.241	.9	.2
11	111	Bottom	.555	.9	.2
12	112	Top	.417	.9	.2
13	113	Front Reflector	.34722	.05	.2
14	114	Front Radiator	.11111	.9	120
15	115	Front Mask	.16667	.9	10^{-3}
16	116	Rear Mask	.16667	.9	10^{-3}
17	117	Rear Radiator	.11111	.9	120
18	118	Rear Reflector	.34722	.05	.2
19	119	Thermal Bag	.173	.02	10^{-3}
20	120	Thermal Bag	.137	.02	10^{-3}
21	121	Thermal Bag	.137	.02	10^{-3}
22	122	Thermal Bag	.346	.02	10^{-3}
23	123	Thermal Bag	.137	.02	10^{-3}
24	124	Thermal Bag	.137	.02	10^{-3}
25	125	Thermal Bag	.396	.02	10^{-3}
26	126	Thermal Bag	.137	.02	10^{-3}
27	127	Thermal Bag	.162	.02	10^{-3}
28	128	Thermal Bag	.162	.02	10^{-3}
29	129	Front Masked Rad.	.167	.9	120
30	130	Rear Masked Rad.	.167	.9	120
99	---	Lunar Surface	---	--	---
100	---	Deep Space	---	--	---

3.3.3.1 Conductivity of HFE Structure and Insulation

The outer shell of the HFE, i.e. the sunshield, reflector mask, covers, etc. is made from a glass fiber low pressure, epoxy resin laminated plastic material, Type II class 1, fabric number 120 per mil standard MIL-P-25421. The epoxy resin is Shell Epon 826 with curing agent "Z". A fiberglass thermal conductivity of 0.2 Btu/hr/ft°F was assumed.

For the multilayer insulation, an effective normal conductivity of $k = 1.0 \times 10^{-3}$ Btu/hr/ft°F was assumed. For heat flow parallel to the bag sides a value of $k = 1.0 \times 10^{-2}$ Btu/hr/ft°F was assumed. The effect of mask thermal conductivity on average thermal plate temperature is presented in Figure 3.7.

3.3.4 Electronic Power Dissipation

The effect of electronic power dissipation was included in the analysis by means of a table heat input to the four thermal plate nodes (nodes 14, 17, 29, 30). The power was assumed to be uniformly distributed on the plate. Hence, the amount of power received by each node was determined by the ratio of the area of the respective node to the total thermal plate area. For lunar noon conditions a power dissipation of 3.8 watts was used for all deployment latitudes. In the lunar night condition a value of 9.3 watts was used. Several other electronic power values were used in order to determine the sensitivity of the average thermal plate temperature to changes in power output levels as mentioned in section 3.2.4. The distribution of power for the thermal plate nodes is indicated in Table 3.2 for several cases considered.

3.3.5 Lunar Surface Temperatures

The variation of lunar noon surface temperature with latitude is indicated in Figure 3.8. These values of lunar surface temperature were used for the respective latitudes and the temperatures input to the lunar surface node (node 99). For lunar night conditions a surface temperature of -300°F was used for all deployment latitudes.

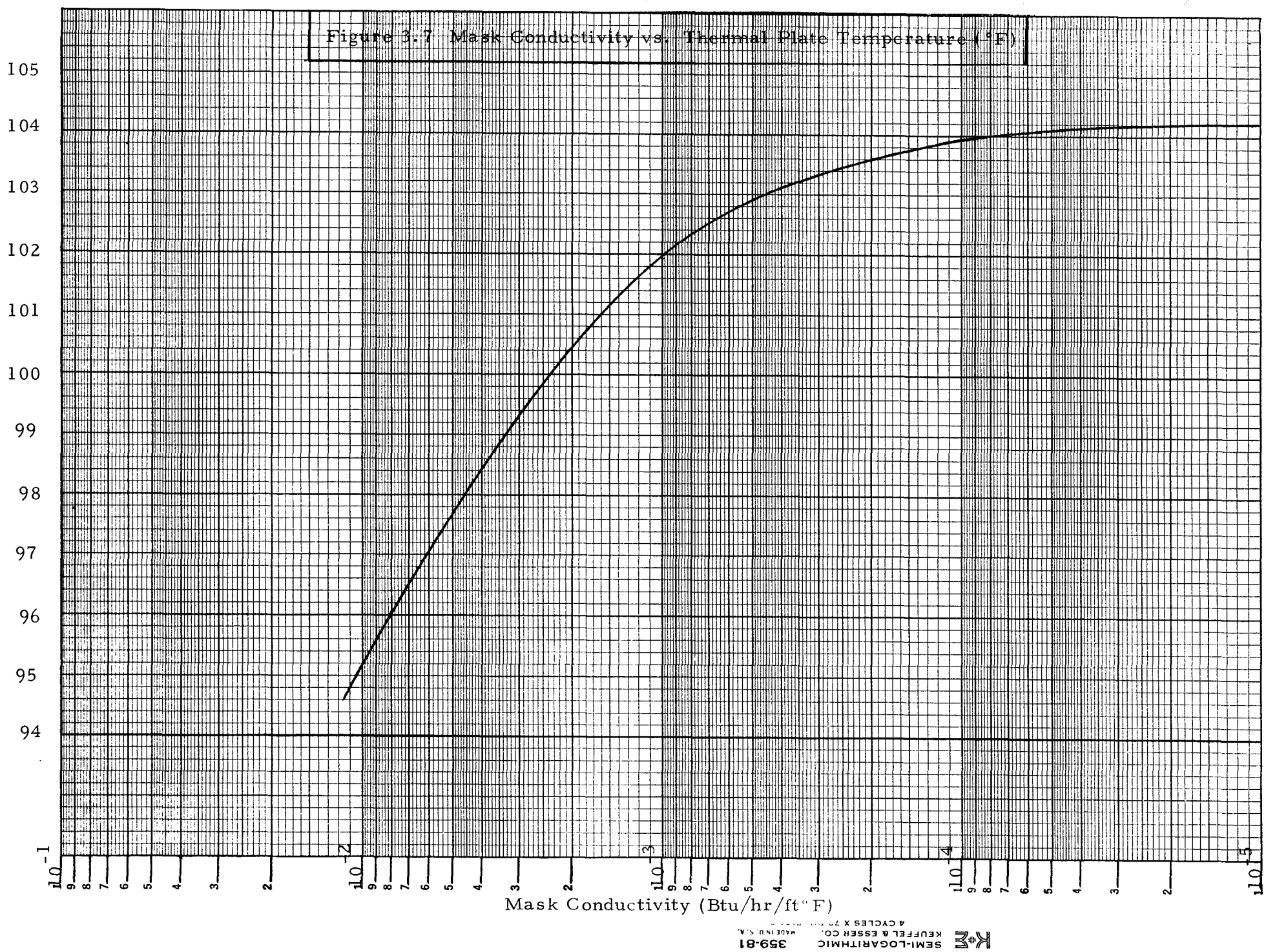
Figure 3.7 Mask Conductivity vs. Thermal Plate Temperature (°F)
105
104
103
102
101
100
99
98
97
96
95
94
10^{-1}
10^{-2}
10^{-3}
10^{-4}
10^{-5}
Mask Conductivity (Btu/hr/ft² °F)
359-81
SEMI-LOGARITHMIC
KEUFFEL & ESSER CO.
MADE IN U.S.A.
4 CYCLES X 70

TABLE 3.2

ELECTRONIC POWER DISSIPATION - WATTS

Node	Power (Watts)				Comment
	3.8 (1*)	6.	9.3 (2**)	10.	Total Power Watts
14	0.758	1.199	---	1.998	Lunar Noon
17	0.758	1.199	---	1.998	
29	1.138	1.797	---	2.996	
30	1.138	1.797	---	2.996	
14	0.758	1.199	1.858	---	Lunar Night
17	0.758	1.199	1.858	---	
29	1.138	1.797	2.787	---	
30	1.138	1.797	2.787	---	

*1 Lunar noon values used in analysis corresponding to mode I operation

**2 Lunar night values used in analysis corresponding to ALSEP Flight 3 nominal power dissipation

Figure 3.8 Variation of Lunar Noon Surface Temperature with Deployment Latitude

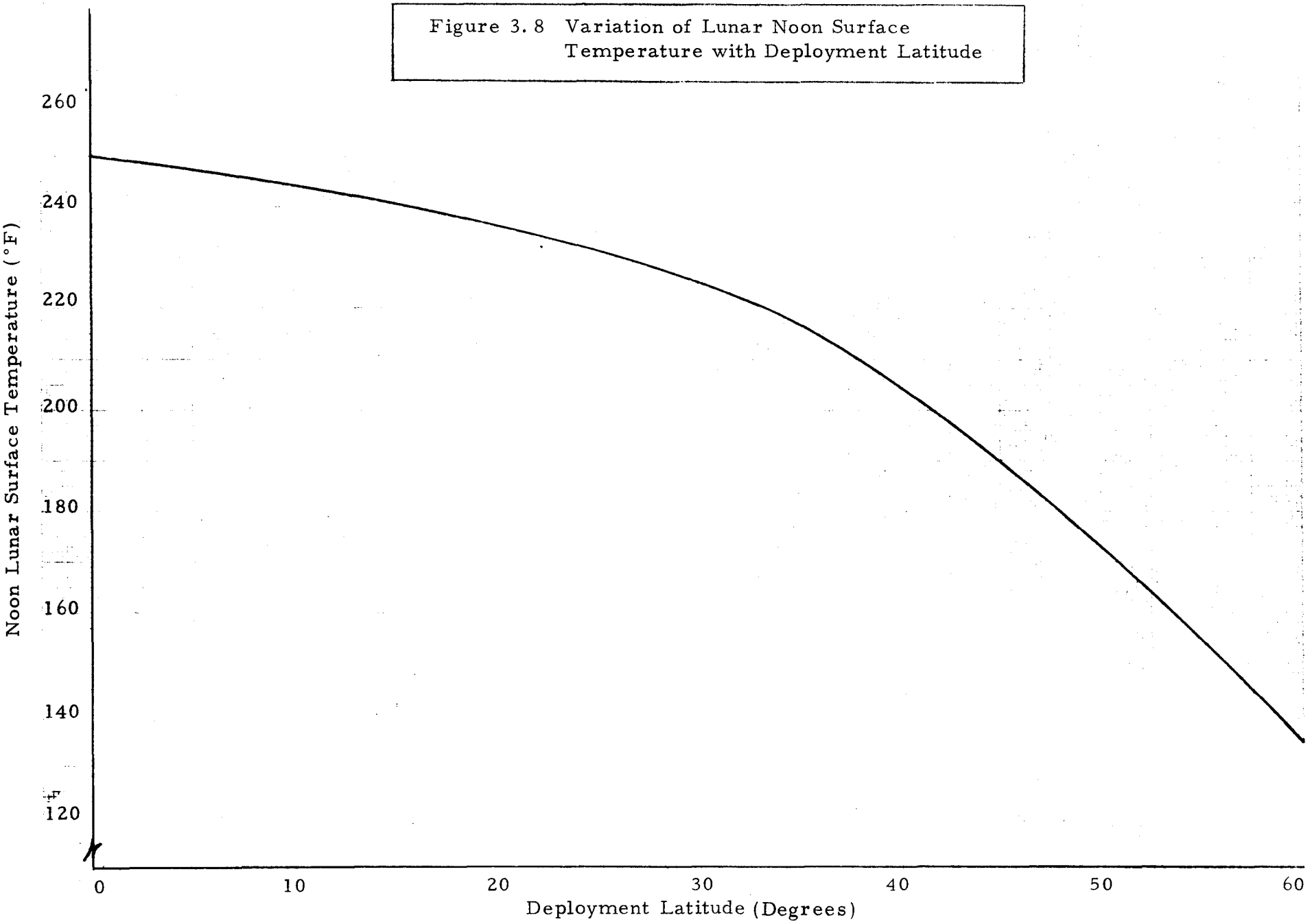

In the case of the lunar sunrise simulation two lunar surface temperatures were used (250°F and -300°F) to bracket the possible temperature range. It is expected that the actual lunar surface temperature will be nearer to -300°F than 250°F and hence serves as a more realistic estimate of component temperatures.

3.3.6 Surface Degradation

To simulate the effects of varying amounts of lunar dust covering the HFE, the numerical value of the solar absorptance was increased from the nominal value of α_s = 0.20 to 0.6 and 0.9. This corresponds to 0, 50 and 100% dust coverage.

3.3.7 Solar Heating

3.3.7.1 Lunar Noon Condition

The deployment latitude determines the areas of thermal control surfaces which are directly illuminated and the intensity of the incident flux. Table 3.3 presents the individual surfaces illuminated as a function of deployment latitude. The values used for solar heating are presented in terms of the amount of dust coverage and deployment latitude in Table 3.4 for lunar noon.

3.3.7.2 Lunar Sunrise Condition

To simulate the effects of a lunar sunrise, three deployment latitudes were chosen for analysis: 5°, 10°, and 16°45'. The later serves as the limiting case in which the maximum area is directly illuminated for the reflector and side curtains.

The effect of reflection of incident energy by the specular reflectors was calculated by means of ray tracing. The values obtained for the flux absorbed due to reflections from other surfaces were negligible for the 5° and 10° latitude but were included in the values used for the 16°45' case although they are only approximately 10% of the direct value. The resulting absorbed solar fluxes are listed in Table 3.5 as a function of deployment latitude.

TABLE 3.3

DIRECT ILLUMINATION OF COMPONENTS AS A FUNCTION OF DEPLOYMENT LATITUDE

Deployment Latitude (Degrees)	Directly Illuminated Nodes
0	12, 16*, 15*
15	12, 9, 15*
30	12, 9, 15, 14*
45	12, 9, 15, 14, 13
60	12, 9, 15, 14, 13

*Node only partially illuminated directly

NOTES:

1. At all latitudes greater than 14° 2' node 16 is not illuminated.
2. At all latitudes greater than 19° 18' node 15 is totally illuminated.
3. At all latitudes greater than 36° 52' the base radiator plate is totally illuminated.
4. At all latitudes greater than 36° 52' the specular reflector is illuminated. This is a case of either total illumination or none at all.

TABLE 3.4

ABSORBED SOLAR FLUX AT LUNAR NOON (Btu/hr)

Nominal Surface Properties $\alpha = 0.2$

Node	Node Description	Latitude (Degrees) 0	15	30	45	60
14	Radiator	.26	.5212	6.3	10.64	8.58
17	Radiator	.26	0.0	0.0	0.0	0.0
1	Side Curtain	.1213	.2437	.4589	.7856	.7019
3	Side Curtain	.1213	0.0	0.0	0.0	0.0
5	Side Curtain	.1213	.2437	.4589	.7856	.7019
7	Side Curtain	.1213	0.0	0.0	0.0	0.0
9	Front	0.0	5.524	10.672	15.092	19.48
12	Top	36.911	35.786	31.968	26.096	18.46
13, 18*	Reflector	.2717	.5457	.9318	9.96	17.68
15, 16**	Mask	6.81	13.762	14.878	16.14	13.28

Degraded (50% Dust) - $\alpha = 0.6$

Node	Node Description	Latitude (Degrees) 0	15	30	45	60
14	Radiator	.13	.26	15.273	22.739	16.596
17	Radiator	.13	0.0	0.0	0.0	0.0
1	Side Curtain	.06	.12	.229	.393	.35
3	Side Curtain	.06	0.0	0.0	0.0	0.0
5	Side Curtain	.06	.12	.229	.393	.35
7	Side Curtain	.06	0.0	0.0	0.0	0.0
9	Front	0.0	16.573	32.015	45.277	55.251
12	Top	110.73	107.36	95.894	78.29	55.451
13, 18*	Reflector	.135	.27	.466	26.71	32.448
15, 16**	Mask	18.456	37.78	39.40	34.16	25.098

Degraded (100% Dust) $\alpha = 0.9$

Node	Node Description	Latitude (Degrees) 0	15	30	45	60
14	Radiator	--	--	21.842	31.350	22.171
17	Radiator	--	--	--	--	--
1	Side Curtain	--	--	--	--	--
3	Side Curtain	--	--	--	--	--
5	Side Curtain	--	--	--	--	--
7	Side Curtain	--	--	--	--	--
9	Front	--	24.884	48.071	67.983	83.260
12	Top	166.261	161.199	143.981	117.54	83.133
13, 18*	Reflector	--	--	--	39.162	47.968
15, 16**	Mask	27.713	55.666	57.599	47.016	33.270

*18 only directly illuminated at 0 degrees latitude
**16 only directly illuminated at 0 degrees latitude

TABLE 3.5

ABSORBED SOLAR FLUX-LUNAR SUNRISE CONDITION* (Btu/hr)

Latitude	Surfaces					
	1, 3	2	4	9	5	13
5°	3.70	7.32	16.9	1.9	.93	.17
10°	3.69	7.24	16.75	3.72	1.47	.73
16°45'	3.54	7.04	16.47	6.15	1.89	2.39

*Nominal surface properties (α = 0.2)

3.4 TEST RESULTS

3.4.1 EPA Test Results

The results of the HFE EPA (Electronics Package Assembly) BxA ALSEP series of thermal/vacuum tests have been summarized with the exception of the ETV* performed at the Beech Aircraft facilities with the 8-inch wide sunshield design. These results are not included since the sunshield configuration differs from the final sunshield configuration (i.e., the 6-inch wide sunshield).

A summary of the general test conditions for the 6-inch sunshield HFE EPA thermal/vacuum test series is presented in Table 3.6. The BxA ALSEP series of tests includes the (1) MSC ETV*, (2) DVTV*, (3) QATV-SB, and (4) FATV-3. This table shows the method of solar simulation, the number of solar constants, the thermal control coating properties and source. Carbon arc lamps were used during the MSC ETV to simulate the solar energy impinging on the external surfaces. These lamps approximate the spectral distribution of the solar flux. All other tests were performed with infrared quartz lamps which simulate the heat loads absorbed on the external surfaces of the HFE EPA. As a result, the spectral reflectance of the irradiated surfaces and the spectral flux of the lamps must be known accurately for an adequate simulation.

The HFE EPA thermal model tested at MSC was coated with the Ball Brothers'63 W white thermal control coating for the nominal surface condition and with the 3M company's 401-C10 black thermal control coating for the degraded surface condition. All other tests simulated surface degradation by increasing the intensity of the quartz lamps. During the DVTV the intensity of the lamps was increased to four solar constants to simulate total degradation of the exterior surfaces. Total degradation, as implied by the ALSEP program, includes vacuum-radiation effects and lunar dust particles such that the effective solar absorptance of the surface degrades to $\alpha_s = 0.9$ or the ratio of solar absorptance to infrared emittance $\alpha_s/\epsilon_{ir} = 1.0$.

---

*NOTE: 1. These Tests were performed per test plans and procedures in Refs. 17 to 21.

TABLE 3.6

SUMMARY OF HFE THERMAL/VACUUM TEST CONDITIONS AND CONFIGURATIONS

T/V Test	Solar Simulation		Thermal Coating		Lunar Surface Temperature (F°)		Radiator Area ft.2	Bolted to Lunar Surface	Probe Cable Tray	Guide Cups
	Method	Solar Constants	Source	Properties (α_s/ϵ_{IR})	Noon Spec. (actual)	Night				
1. MSC Eng.	carbon arc lamps	1.0	63w Ball Brothers	.24/.84	250 ± 10	-240 ± 20 (-235.0)	27.45	Yes	No	No
2. DVTV	Quartz lamps	1.0/4.0	3M-401-C10 IITRI (S-13G)	.9/.9 .2/.9	250 ± 10	-300 ± 10 (-320.0)	30.85	No	No	No
3. QATV-SB	Quartz lamps	1.25	IITRI (S-13G)	.2/.9	280 ± 10 (289.16)	-300 ± 10 (-301.87)	30.85	No	No	No
4. FATV-3	Quartz lamps	1.0	IITRI (S-13G)	.2/.9	250 ± 10	-300 ± 10 (-314.0)	30.85	No	Yes	Yes

The intensity of the lamps was increased to 1.25 solar constants in the QATV-SB. This intensity represents the presently expected surface degradation in solar absorptance of highly reflective thermal control coatings. In addition, the lunar surface simulator was increased from 250. ± 10°F to 280. ± 10°F to simulate possible local hot areas. These two conditions represent the ALSEP design limits. The FATV-3 was performed with the nominal ALSEP lunar environment of 1 solar constant and the lunar surface simulator set at 250. ± 10°F.

All models of the HFE EPA were coated with IITRI S-13G thermal control coating. The one exception was the thermal model used during the MSC ETV. This model was coated with Ball Brothers 63W white to evaluate the adhesion of this thermal control coating to non-metallic substrates.

During the previous test at Beech Aircraft this model, which was coated with IITRI S-13 thermal control coating, experienced loss of adhesion during the cold portion of the thermal/vacuum cycle. The Ball Brothers thermal control coating was also found to fail in adhesion. To remedy this difficulty, tests were run on coupons at IITRI to evaluate the application process specifications on the S-13G thermal control coating. An adequate process was found and applied to subsequent models. (Ref. 15)

The lunar surface simulator in each thermal/vacuum test was cycled from 250. ± 10°F to -300. ± 20. °F which represents the nominal ALSEP specifications. Two exceptions were the MSC ETV and the QATV-SB. During the MSC ETV the lunar surface simulator was not connected to the LN_2 flow. The cooling of this surface was by radiation to the cold surroundings and by the small amount of conduction along the supports. As a consequence, the lunar surface simulator would have taken a longer period of time than was practical to reach the ALSEP specifications and possibly never reach the required temperatures due to heat sources such as the quartz windows, conduction along supports, etc. Thus, the lunar night surface specifications were changed for this test only to -240. ± 20. °F. The QATV-SB was performed with the lunar surface simulator at the ALSEP design limit condition of 280. ± 10. °F for the lunar noon condition.

The effective radiator area of the final HFE EPA configuration is 30.85 in^2. The thermal model used in the MSC ETV had an effective radiator area of 27.45 in^2. This smaller radiator area increases the stabilization temperature of the electronics at thermal equilibrium. The temperature increase of the HFE EPA would tend to occur more at night than during the day with the smaller radiator area; thus, decreasing the lunar noon-night temperature excursion.

The HFE EPA was bolted to the lunar surface simulator via the mounting tabs* during the MSC ETV since the surface was vertical in order to be in line with the carbon arc solar simulator and in order to be rotable. As a consequence, there was a direct conduction path from the lunar surface simulator to the mounting tabs which are integral with the isolation ring. The probe cable tray and the Boydbolt guide cups were mounted on the FATV-3 model to simulate the actual flight configuration as accurately as possible (see reference 11, 13 and 14).

The adequacy of the lunar surface simulation has been previously reported in references 12 and 16. The values reported in these two references have been recomputed more precisely and are presented in table 3.7. Table 3.7 presents the geometric configuration factors from the external surfaces (i.e., nodal areas) of the HFE EPA to the MSC ETV, DVTV, QATV-SB and FATV-3 lunar surface simulators. The factors have been computed on the CONFAC II computer program for both the direct views and the views as seen through the specular reflector. These values are compared to the actual lunar surface values which were also precisely computed by machine.

The effect of other equipment on the lunar surface simulators in the DVTV, QATV-SB and FATV-3 has not been included in this study due to its complexity. The MSC ETV being an engineering test did not have any other equipment on the lunar surface simulator, thus the values are accurate. The effect of nonuniformity of the surface simulator temperature and the nonuniformity of the vertical lip heights in the MSC ETV, QATV-SB and FATV-3 have not been studied.

NOTE: * There were 3 mounting tabs on the thermal model vs. 4 mounting tabs on all subsequent models.

The results in table 3.7 show an improvement in simulation from the MSC ETV to the DVTV and a considerable improvement from the DVTV to the QATV-SB and FATV-3 due primarily to the addition of vertical lips about the edges of the lunar surface simulator. However, the view of the surface simulator as seen by the radiator through the specular reflector is moderately oversimulated.

This condition could be realized if the HFE is deployed in a lunar depression or in the vicinity of lunar rocks and/or geological formations of higher elevation such as crater ridges, hills and plateaus.

The internal power dissipation is reported in reference 10 for the QATV-SB EPA. Internal power dissipation for all other EPA models were obtained informally.

Tables 3.8 through 3.11 present the results of the MSC ETV to the FATV-3. Notes are also shown on each table to facilitate comparison between tests. Table 3.8 presents the average temperature of the HFE EPA radiator plate for (1) the nominal and degraded lunar noon, (2) the lunar morning and after noon at 45° solar angle, (3) the lunar noon (when the HFE EPA is misaligned with the vertical by 17°), and (4) the lunar night conditions as a function of internal power dissipation. The internal power dissipation for this test of 2.8 W, 6.0 W and 8.8 W correspond respectively to the values of (1) the survival power, (2) the expected day time power consumption and (3) the total power allotted to the experiment at the time of the test. The total power includes the EPA operational power and the heater power available which corresponds to the power required for lunar night operation.

The lunar noon degraded condition was performed to verify that the HFE EPA would perform within the operating temperature limits if total degradation did occur during the ALSEP mission. This surface condition was accomplished by removing the high solar reflective 63W white thermal control coating and coating the HFE EPA with 3M-401-C10 black thermal control coating. Table 1 shown that at the 6.0 W conditions (i.e., the max. expected day operation power level) the HFE EPA radiator would exceed the upper operating limit.

TABLE 3.7

GEOMETRIC CONFIGURATION FACTORS FROM HFE NODES TO LUNAR SURFACE SIMULATORS AND SPACE

HFE Surfaces (nodes)	MSC ETV	DVTV	QATV-SA and FATV-3	Actual Lunar Surface	% Difference From Actual		
					MSC ETV	DVTV	QATV-SB FATV-3
Direct View							
Triangle 1	.06013	.06449	.07977	.07565	-20.5	-14.8	5.45
	(.20773)	(.20336)	(.18808)	(.19200)	(8.08)	(5.81)	(-2.14)
Triangle 2	.06012	.05833	.08200	.07565	-20.5	-22.9	8.39
	(.20773)	(.20952)	(.18585)	(.19220)	(8.08)	(9.01)	(-3.30)
End 1	.49830	.46616	.53714	.50	-.34	-6.8	7.4
	(.50170)	(.53384)	(.46286)	(.50)	(.34)	(6.8)	(-7.4)
End 2	.49830	.47928	.50997	.50	-.34	-4.1	2.0
	(.50170)	(.52072)	(.49003)	(.50)	(.34)	(4.1)	(-2.0)
Reflector	.21426	.24895	.28085	.27733	-22.7	-10.2	1.27
	(.26054)	(.22585)	(.19395)	(.19747)	(31.94)	(14.4)	(-1.78)
Side	.58105	.48716	.54484	.50	16.2	-2.6	8.97
	(.41895)	(.51284)	(.45516)	(.50)	(-16.2)	(2.6)	(-8.97)
Radiator*	0.	0.	.00069**	0.	0.	0.	0.
	(.21319)	(.21319)	(.21250)	(.21319)	(0.)	(0.)	(-.32)
Insulated Surface*	0.	0.	.00084**	0.	0.	0.	0.
	(.46871)	(.46871)	(.46871)	(.46871)	(0.)	(0.)	(-.18)
View as seen through reflector							
Triangle	.06529	.08069	.09314	.09210	29.1	-12.4	1.13
	(.13250)	(.11710)	(.10465)	(.10569)	(25.4)	(10.8)	(-.98)
Triangle 2	.06529	.07566	.09211	.09210	-29.1	-17.9	.01
	(.13250)	(.12223)	(.10578)	(.10579)	(25.4)	(15.5)	(-.09)
Radiator	.03650	.03405	.05786	.04439	-17.8	-23.3	30.3
	(.32260)	(.32505)	(.30124)	(.31471)	(2.51)	(3.29)	(-4.28)
Insulated Surface	.08906	.11935	.14359	.13578	-34.4	-12.1	5.75
	(.19909)	(.16880)	(.14456)	(.15237)	(30.7)	(10.8)	(-5.13)

NOTES:
1. Numbers in parenthesis are factors to space
2. * Included only when lip of lunar surface simulator directly views these surfaces
3. ** Effect of blockage not included

The lunar morning and/or afternoon at a 45° solar angle was performed to establish that the lunar noon condition will result in the highest temperatures on the HFE EPA radiator plate. This assumption is shown to be correct in table 3.8.

The 17° misalignment condition was performed to verify that the HFE EPA radiator plate will be maintained within the upper operating temperature limits. At the 6.0 W internal power condition, it was found again that the HFE EPA radiator plate would exceed the upper operating limit. This misalignment condition is the result of the ALSEP mission constraint and tolerance which includes (1) the possibility of ALSEP deployment at ±5° from the lunar equator and/or subsolar path, (2) ±12° leveling tolerance on the HFE EPA.

Tables 3.9 and 3.10 present the results of the DVTV and QATV-SB respectively for each condition tested. These tables present the HK (housekeeping data) for comparison with the thermocouple data. The thermocouple data is presented as the highest and lowest recorded temperature on the HFE EPA radiator plate. During the DVTV experiment modes I and III, corresponding to the gradient and high conductivity tests of the HFE, were performed during the lunar morning conditions. The noon condition was performed with mode III. Since the electronics dissipate the most power at this time, it is thus the worst case during this portion of the lunar cycle. The night condition was performed with the experiment in mode I (i.e., the lowest power condition) to simulate the worst case for the lunar night operation. While the chamber was at the lunar night condition, the experiment was turned to the survival mode of operation to establish whether the experiment could survive the lunar night if inoperative.

The temperature excursion between lunar day (mode III degraded) and lunar night (mode I) is presented. Only one of the thermocouples was found to exceed (only slightly) the required specification of 90°F (i.e., 50°C). The excursion of the HK temperature sensor was well within the requirement.

The QATV-SB results are presented for the lunar noon, night and survival conditions. In this test the noon conditions correspond to the ALSEP design limit conditions. The temperature excursion of both the thermocouples and the HK temperature sensor on the radiator plate were

TABLE 3.8

MSC THERMAL/VACUUM TEST RESULTS OF HFE ENGINEERING TEST MODEL

POWER (watts)	NOON (Nominal) °F (°C)	NOON (Degraded) °F (°C)	45° SOLAR ANGLE °F (°C)	17° Misalignment °F (°C)	NIGHT °F (°C)
2.8	108. (42.5)	120. (48.9)	83. (78.3)	118. (47.8)	-62.0 (-52.2)
6.0	143. (61.8)	150 (65.5)	122. (50.)	150. (65.5)	24 (-0.4)
8.8	167. (75.0)	180 (82.3)	155. (68.3)	173. (78.4)	75 (23.9)

NOTES:

1. Radiator area = 27.45 In^2
2. Model bolted to lunar surface
3. Lunar surface 250. ± 10 °F to -240. ± 20 °F
4. Solar simulation (carbon arc lamp) = 1 solar constant
5. Thermal coating (α_s/ϵ_{IR} = .24/.84-nominal)
   (α_s = 0.9 - Degraded)

TABLE 3.9

HFE DVTV THERMAL/VACUUM TEST RESULTS

THERMOCOUPLES	MORNING °F (°C)	DAY	NIGHT (8.3W)	SURVIVAL
1. Mode 1 (Nominal) (3.86W)	88.7 (31.5) 81.1 (27.3)		29.7 (-1.3) 36 (2.2)	
2. Mode 1 (Degraded) (3.86W)	117.2 (47.4) 109.4 (43.)			
3. Mode III (Degraded) (4.63W)	123.5 (50.9) 116.9 (47.2)	121.4 (49.7) 112.9 (45.0)		
4. Survival Mode (3.2 (3.2W)				-66.0 (-54.5) -59.4 (-50.7)
HK DATA				
1. Mode 1 (Nominal) (3.86W)	87.0 (30.0)		36.4 (2.5)	
2. Mode 1 (Degraded) (3.86W)	113.0 (45.0)			
3. Mode III (Degraded) (4.63W)	120.2 (49.0)	116.0 (47)		

Δ T Between Day (Mode III Degraded) to night (Mode 1)

THERMOCOUPLE DATA	91.7 (50.9) 76.9 (42.8)
HK DATA	79.5 (44.5)

NOTES:

1. HFE SN01 Electronics
2. Radiator area = 30.85 IN^2
3. Solar Simulation (infrared quartz lamps)
4. Lunar Surface (250 ± 10°F to -300 ± 20°F)
5. Thermal coating (α_s/ϵ_{IR} = 0.2/0.9 - Nominal (α = 0.9 Degraded)

TABLE 3.10

HFE QATV-SB THERMAL/VACUUM RESULTS

	NOON (3.78W)	NIGHT (8.3W) °F (°C)	ΔT - NOON-NIGHT	SURVIVAL (3.8 W)
HK DATA	132.0 (55.5)	38.0 (3.3)	94.0 (52.2)	
Thermocouple	132.8 (56)	33.6 (0.9)	99.2 (55.1)	-57.9 (-50.0)
Data	130.4 (54)	37.0 (2.8)	93.4 (51.2)	-52.3 (-46.8)

NOTES:

1. HFE SN02 Electronics
2. Radiator Area = 30.85 In^2
3. Surface degradation = 25.% (1.25 solar constants) } Design limit conditions
4. Lunar surface = 280 ± 10 °F to -300 ± 20 °F }
5. Thermal coating ($\alpha_s/\epsilon_{IR} = 0.2/0.9$)
6. Mode I operation only

found to exceed the original required specification of 90°F (i.e., 50°C). This is primarily the result of a better lunar surface simulation (see table 3.7) and the design limit conditions imposed on this test.

The results of the FATV-3 are presented in table 3.11. During this test, only the HK temperature sensor was available since thermocouples cannot be mounted on flight models. The lunar noon and night conditions were both run with the experiment in mode I. The survival mode was not performed on this model since flight hardware was involved. The excursion of the HK temperature is well within the required specification of 90°F.

Figure 3.9 presents the data from tables 3.8 to 3.11 graphically as a function of internal power dissipation. Superimposed are the upper and lower operating and survival limits. Both of the lower temperature limits have changed during the series of tests. The present lower survival limit was established subsequent to the MSC ETV and prior to the DVTV. This was done to assure survivability of the electronic components. Thus, it is evident that the survival power was adequate for the survival temperature limits of -67°F (i.e., -55°C) in effect at the time of the MSC ETV. However, the internal power dissipation of 2.8 watts was not adequate to maintain the electronics above the present survival limit of -58°C (i.e., -50°C) even with the HFE EPA thermal model. As a result, the survival power was increased to 3.2 watts during the DVTV. The additional power again was found to be insufficient. This is primarily due to the difference in thermal plate radiator area between the thermal model and the actual hardware (see table 3.6). The survival power was increased to 3.8 watts for the QATV-SB model and was found to be adequate.

The internal power dissipation for lunar night operation was found to be adequate for the thermal model used in the MSC ETV. Again, however, the DVTV and QATV-SB models were found to exceed the lower operating limit. This is attributed primarily to the larger radiator area and partly to less night operational power than was alotted for the experiment (i.e., 8.2 W vs. 8.8 W). Thus, in an attempt to meet the operational temperature limit an additional watt of power was added to the HFE EPA FATV-3 model. The additional watt was found to increase the HFEEPA radiator plate only 1.9°F (i.e., 1.03°C). The small increase is partially attributed to the Boydbolt guide cups and the probe cable tray which are mounted directly to the isolation ring. These two attachments tend to act like radiators and increase the effective radiator area of the EPA.

TABLE 3.11

HFE FLIGHT #3 THERMAL/VACUUM TEST RESULTS

	NOON (3.76 W)	NIGHT (9.29 W)	NOON-NIGHT °F (°C)
HK DATA	106.4 (41.36)	39.85 (4.36)	66.6 (37.00)

NOTES:

1. HFE SN05 Electronics
2. Radiator area = 30.85 IN^2
3. 1 solar constant
4. Lunar surface @ 250 ± 10°F to -300 ± 20°F
5. Guide cups and probe cable tray mounted
6. Mode I operation only

Figure 3.9
HFE Radiator Plate Temperatures

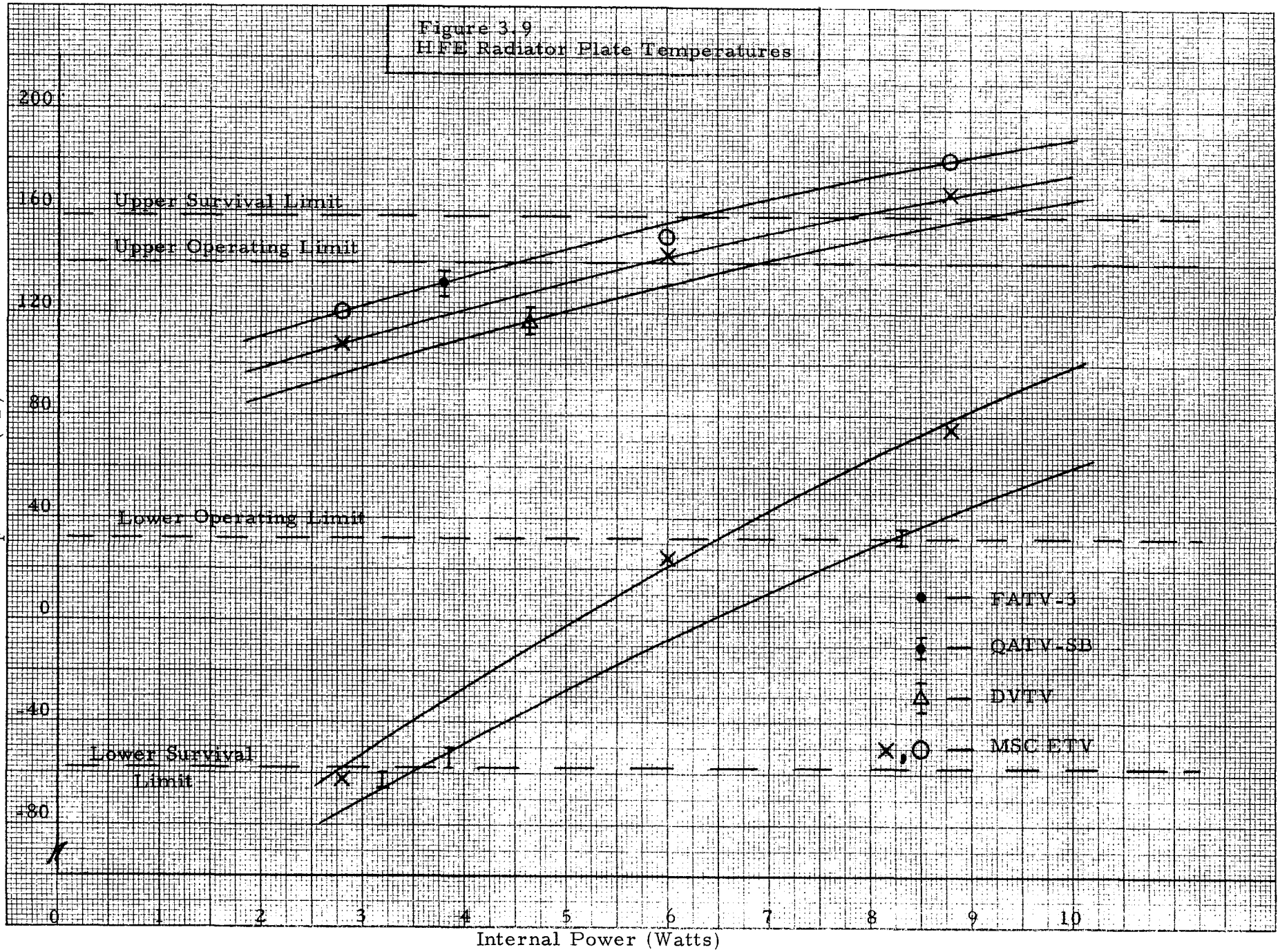

The MSC ETV results for the lunar noon conditions for both the nominal and degraded surface conditions are shown in figure 3.9. For the nominal surface condition the HFE EPA was coated with a white thermal control coating (i.e., Ball Brothers 63 W) with a solar absorptance (α_s) of 0.24.

The degraded surface condition was accomplished by removing the white coating and replacing it with a black thermal control coating (i.e., 3M-401-C10). The QATV-SB model, which had imposed on it the design limit condition, is shown to fall in line with the MSC ETV thermal model for the degraded noon condition. The radiator plate temperature of the FATV-3 model was found to be lower than that of the MSC ETV thermal model for the nominal lunar noon condition This is attributed to (1) the larger radiator area of the FATV-3 model and (2) the lower value of solar absorptance of the thermal control coating on the external surfaces (i.e., α_s = 0.24 of the 63 W and α_s = 0.2 of the S-13 G).

The degraded lunar noon condition of the DVTV model in mode III is shown to fall in line with the FATV-3 model at the nominal lunar noon condition. The primary reasons for this are (1) the better lunar surface simulation in FATV-3 (see table 3.7) and (2) the difference in effect between the design limit condition and the total surface degradation. In the DVTV the infrared quartz lamps used to simulate the solar input were increased in intensity (i.e., 4 solar constants) to simulate the heat loads absorbed on the external surfaces of the HFE EPA. During the QATV-SB, the intensity of the quartz lamps was increased approximately 25% and in addition, the lunar surface simulator was increased from 250°F to 280°F. Thus, the HFE EPA radiator viewed a much hotter lunar surface via the specular reflector in the FATV-3.

Table 3.12 presents items that could affect the thermal control of the HFE EPA thermal radiator plate. This table is presented to reveal what changes could be made to increase the radiator plate temperature above the original operating temperature limit during the lunar night. The expected effect on the thermal control system is shown along with the recommended action that could be taken in the event that the original lower operating limit is required. The only item considered to have a major effect on the thermal control system is the effective radiator size. It is also highly recommended that the Boydbolt guide cups and probe cable tray be positively removed since these two items were never considered in the design of the thermal control system.

TABLE 3.12

ITEMS THAT COULD AFFECT THERMAL CONTROL OF HFE EPA

Item	Influence	Comment
1. Guide cups	Minor	Positive removal by either astronaut or mechanical means
2. Probe cable tray	Minor	Positive removal by either astronaut or mechanical means
3. Gap between apex of specular reflector and		Increase gap to 0.125 ± .01 for both radiator plate and isolation ring.
a. Radiator plate	Minor	
b. Isolation ring	Minor	
4. Radiator masking	Major	Increase mask dimension to 2.50 ± 0.02" (Dwg. 2334630)
5. Gap between edge of radiator and isolation ring	Minor	Assure gap is uniform around circumference of plate
6. Screws that hold probe cable tray	Minor	Replace metal screws by nylon screws
7. Radiative coupling between thermal plate and isolation ring	Minor	Vacuum metalize: 1. the thermal plate on the edges and bottom adjacent to isolation ring. 2. The isolation ring on the inner side.

It became obvious from the DVTV HFE EPA model that the gap between the apex of the specular reflector and the radiator plate was either very small or non-existant. Thus, in the actual flight hardware the radiator plate is either shorted to the sunshield assembly or could be shorted to the sunshield due to thermal distortion of the structure during the extremes of the lunar cycle.

During the DVTV the temperature gradient on the sunshield was 15°F at the lunar noon condition and 69°F at the lunar night condition. During the QATV-SB the temperature gradient across the sunshield was 10°F during the lunar noon condition, 46°F during the lunar night condition and 44°F during the lunar night survival condition further supporting the possibility of thermal shorting of the radiator to the sunshield structure due to thermal distortion.

3.4.2 Thermal Gradients in HFE EPA Circuit Boards

Thermal-vacuum tests of a typical electronic printed circuit board were conducted to determine thermal gradients in the board (reference 8). Fourty 10 ohm resistors were bonded to the board to simulate thermally dissipative components on the actual board. Copper constantan thermocouples were attached to the board at locations shown in figure 3.10. The circuit board was attached to an aluminum heat sink plate by six mounting posts. The entire assembly was then mounted to the baseplate of a Bell jar using a thermally nonconducting material. The vacuum jar was evacuated to 10^{-3} mm mercury and the desired power dissipation on the circuit board was set.

The data presented in table 3.13 was obtained. The temperatures are those measured by thermocouples located as shown in figures 3.10 and 3.11.

For 1.96 watts of power dissiapted on the circuit board, which corresponds to heat dissipated by a typical board in the EPA, the following thermal gradients were determined.

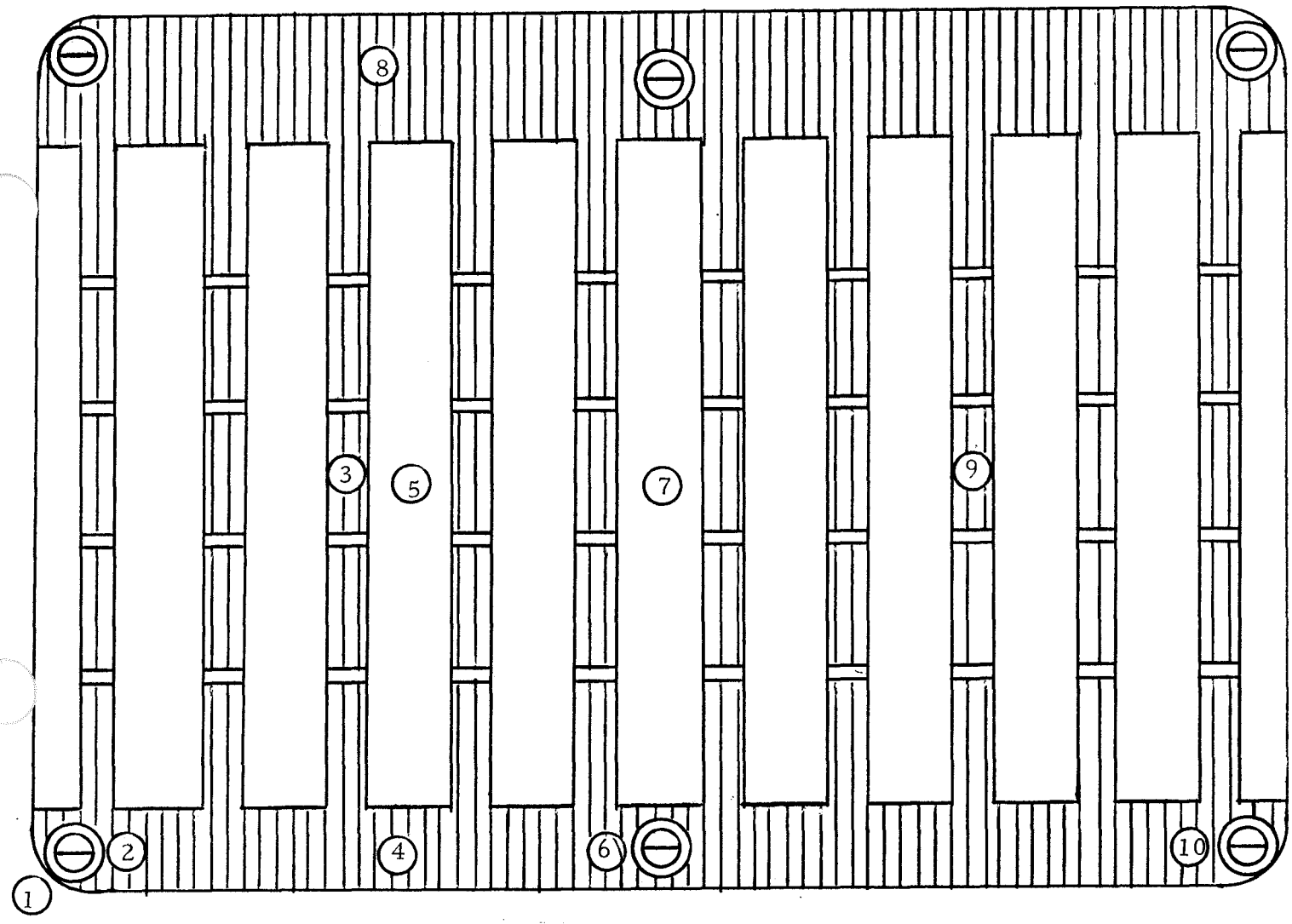

Figure 3-10 Circuit Board Showing Location of Thermocouples

= Copper Conducting Paths

= Epoxy Laminate

= 10 Ohm Resistors

10 = Location of Thermocouples

NOTE: * Thermocouple is mounted on mounting post near thermal control plate (heat sink)

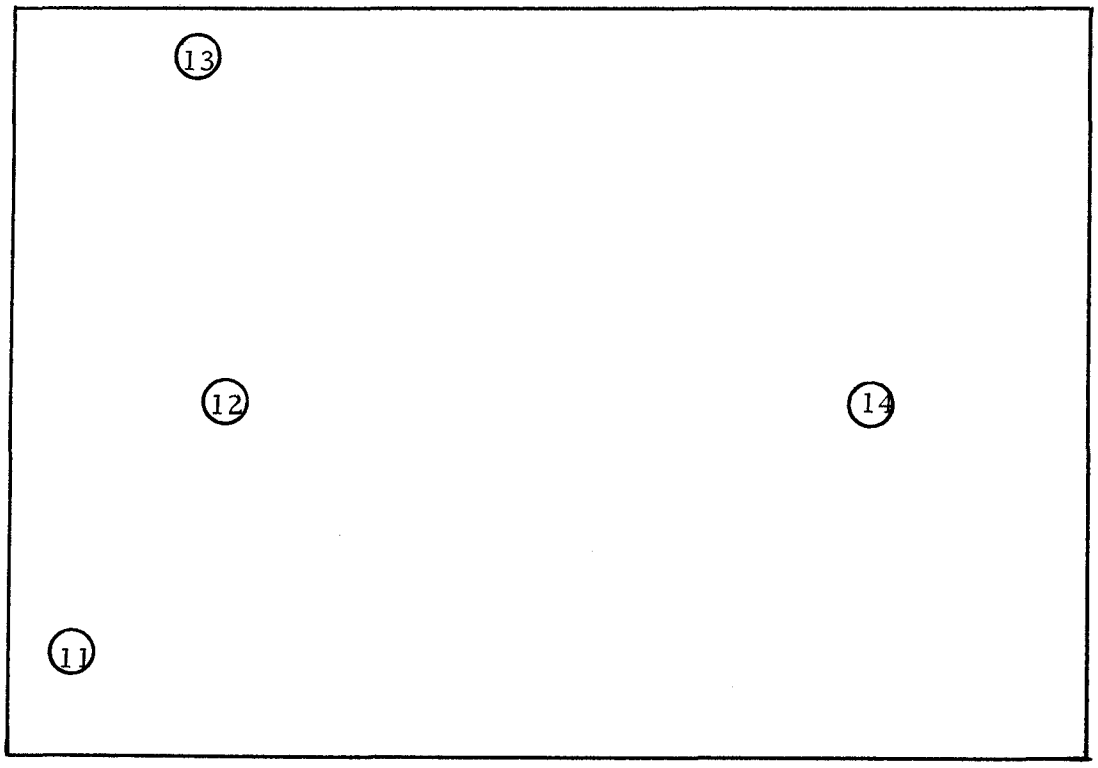

Figure 3-11 Thermocouple Locations On Aluminum Heat Sink Plate

(14) = Thermocouple Locations

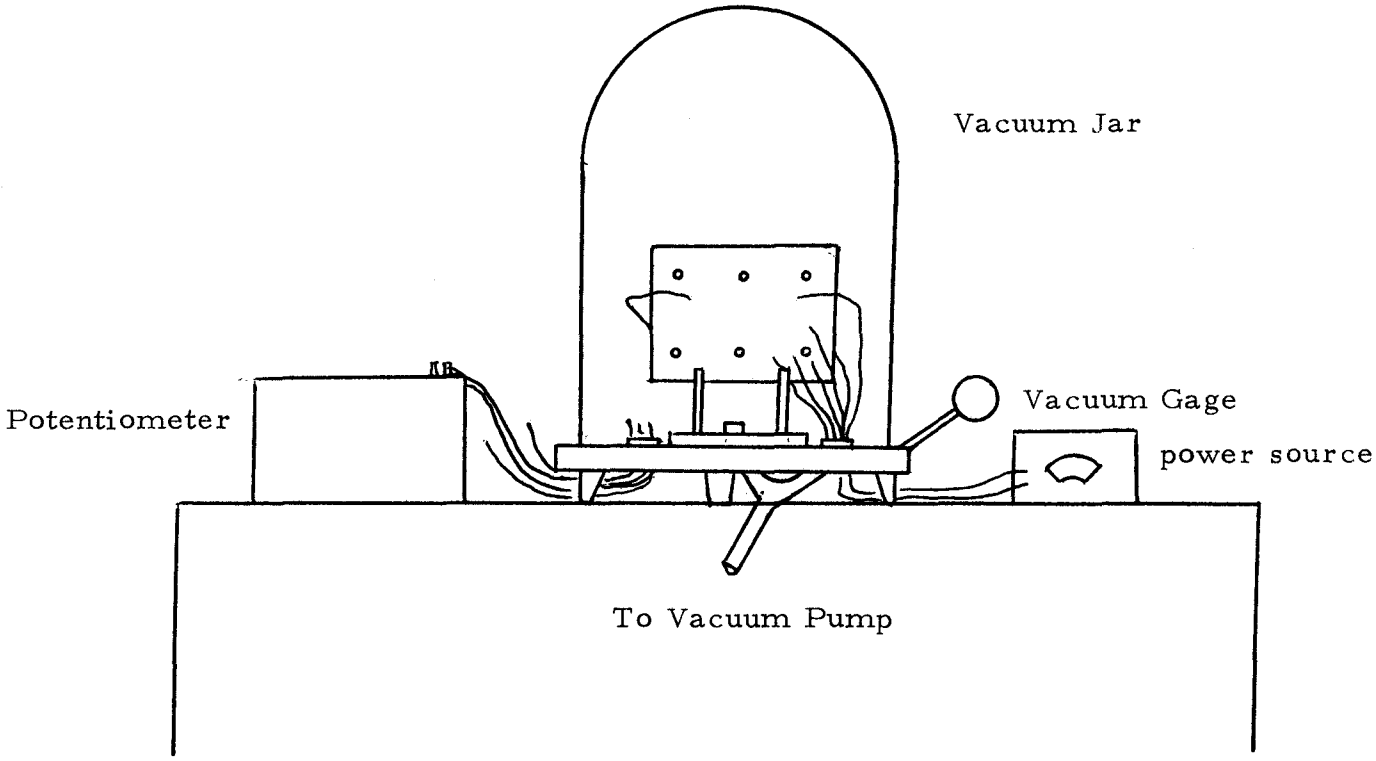

Figure 3-12 Complete HFE Circuit Board Test Assembly

TABLE 3.13

TEMPERATURE GRADIENTS IN HFE ELECTRONICS

Room Temp. (°F)	Press. (mm h_g)	Current (amps)	Pwr. (Watts)	T_1 (°F)	T_2 (°F)	T_3 (°F)	T_4 (°F)	T_5 (°F)	T_6 (°F)	T_7 (°F)	T_8 (°F)	T_9 (°F)	T_{10} (°F)
73.0	10^{-3}	0.100	4.00	96.5	100.4	115.5	105.7	110.4	103.1	110.4			
80.5	10^{-3}	0.070	1.96	88.0	90.4	98.3	93.2	95.9	91.7	95.5			
76.6	10^{-3}	0.070	1.966	85.0	87.8	96.2				93.1	90.5	96.8	88.7

Thermal Gradients on Circuit Board

Room Temp. (°F)	Press. (mm h_g)	Current (amps)	Pwr. (Watts)	T_{11} (°F)	T_{12} (°F)	T_{13} (°F)	T_{14} (°F)	T_9 (°F)	T_2 (°F)	T_7 (°F)
71.6	10^{-3}	0.070	1.96	85.2	85.2	85.2	85.2	95.0	86.5	91.4
74.5	10^{-3}	0.100	4.00	97.7	97.7	97.7	97.7	118.4	102.2	110.7

Temperature Gradients on Heat Sink

ΔT_{2-1}	=	2.4°F	ΔT_{3-4}	=	5.1°F
ΔT_{3-5}	=	2.4°F	ΔT_{3-8}	=	5.7°F
ΔT_{4-6}	=	1.5°F	ΔT_{6-10}	=	3.0°F
ΔT_{9-3}	=	0.6°F	ΔT_{6-2}	=	1.3°F
ΔT_{3-2}	=	7.9°F	ΔT_{9-7}	=	3.7°F
ΔT_{9-10}	=	8.1°F	ΔT_{3-7}	=	3.1°F

It can be seen that the thermal gradients are small and will not cause thermal stress problems in the circuit boards.

No thermal gradients were measured on the aluminum heat sink plate.

From the experimental data it is concluded that excessive thermal gradients do not exist and therefore excessive thermal stresses will be absnet from the EPA circuit boards.

3.5 MODEL CORRELATION

After the initial analytical model was developed, the ALSEP Flight 3 and QATV-SB thermal vacuum tests were correlated. The results of these tests are presented in reference (1). Three cases were considered: (1) lunar night, (2) undegraded lunar noon and (3) noon degraded. Table 3.6 lists the results of the correlations. Since the presence of a lip on the lunar surface simulator alters the view factors from the HFE to the lunar surface and space, different radiation resistors were calculated for the correlation analysis. These values are listed in Appendix 4 and are based on re-calculated view factors to the lunar surface simulator and the cryowall. A temperature of -300°F was used as the deep space temperature of the cryowall sink during the test. During the course of the correlation with the degraded test results.it was discovered that for the QATV-SB tests 1.36 suns rather than 1.25 suns were used in the degraded case and that the temperature of the lunar surface simulation was more nearly 300°F in the area of the HFE than 280°F. The actual distribution of lunar surface temperature is presented in Figure 3.9 for the QATV-SB test and Figure 3.10 for the Flight 3 test. The variation of thermal plate temperature for the HFE in the chamber as a function of lunar simulator average temperature is presented in Figure 3.15.

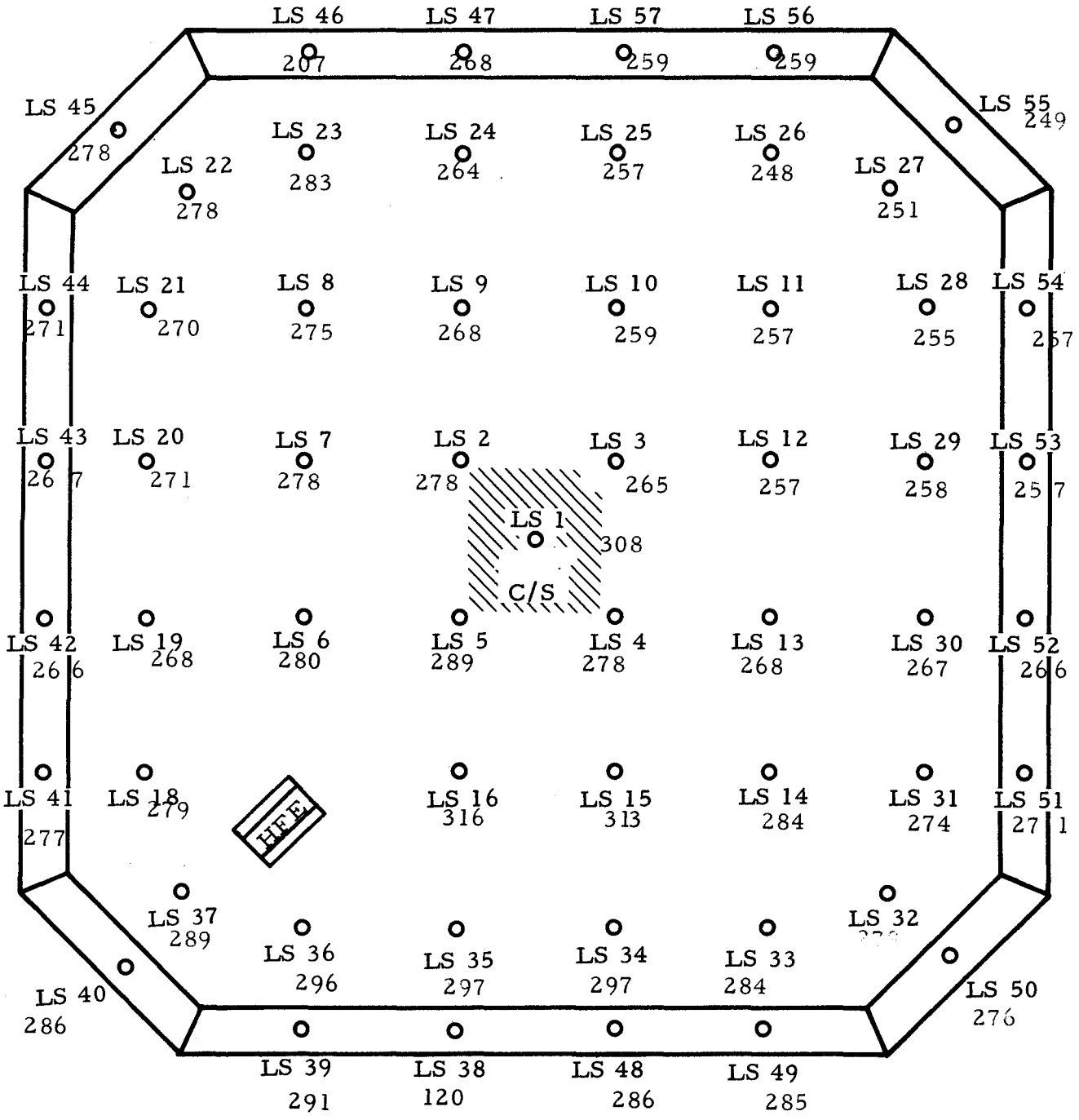

Figure 3.13 Lunar Surface Simulator Temperature Distribution For Qual SB

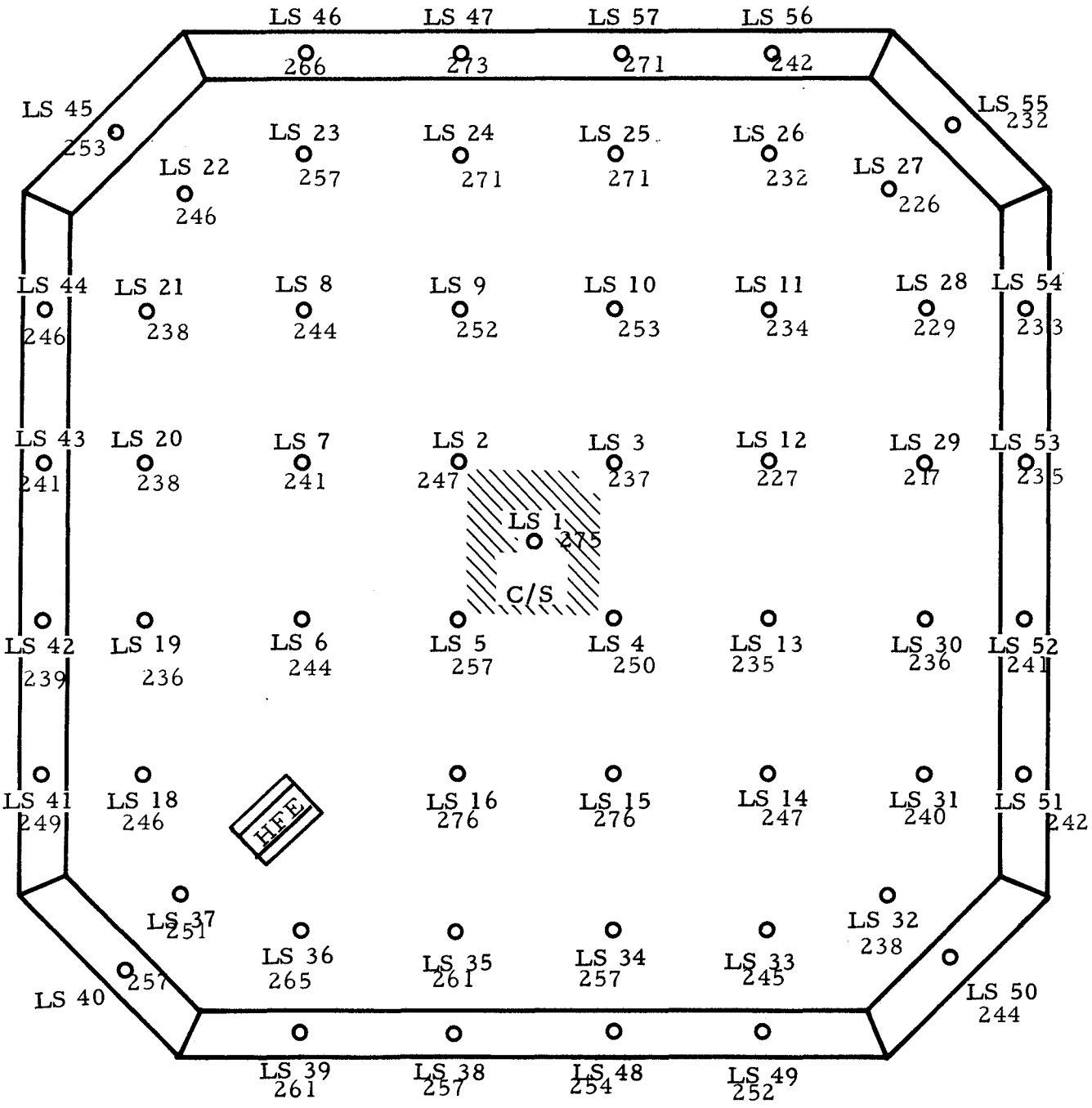

Figure 3.14 Lunar Surface Simulator Temperature Distribution For FLT 3

Figure 3.15 Thermal Plate Temperature vs. Lunar Surface Simulator Temperature

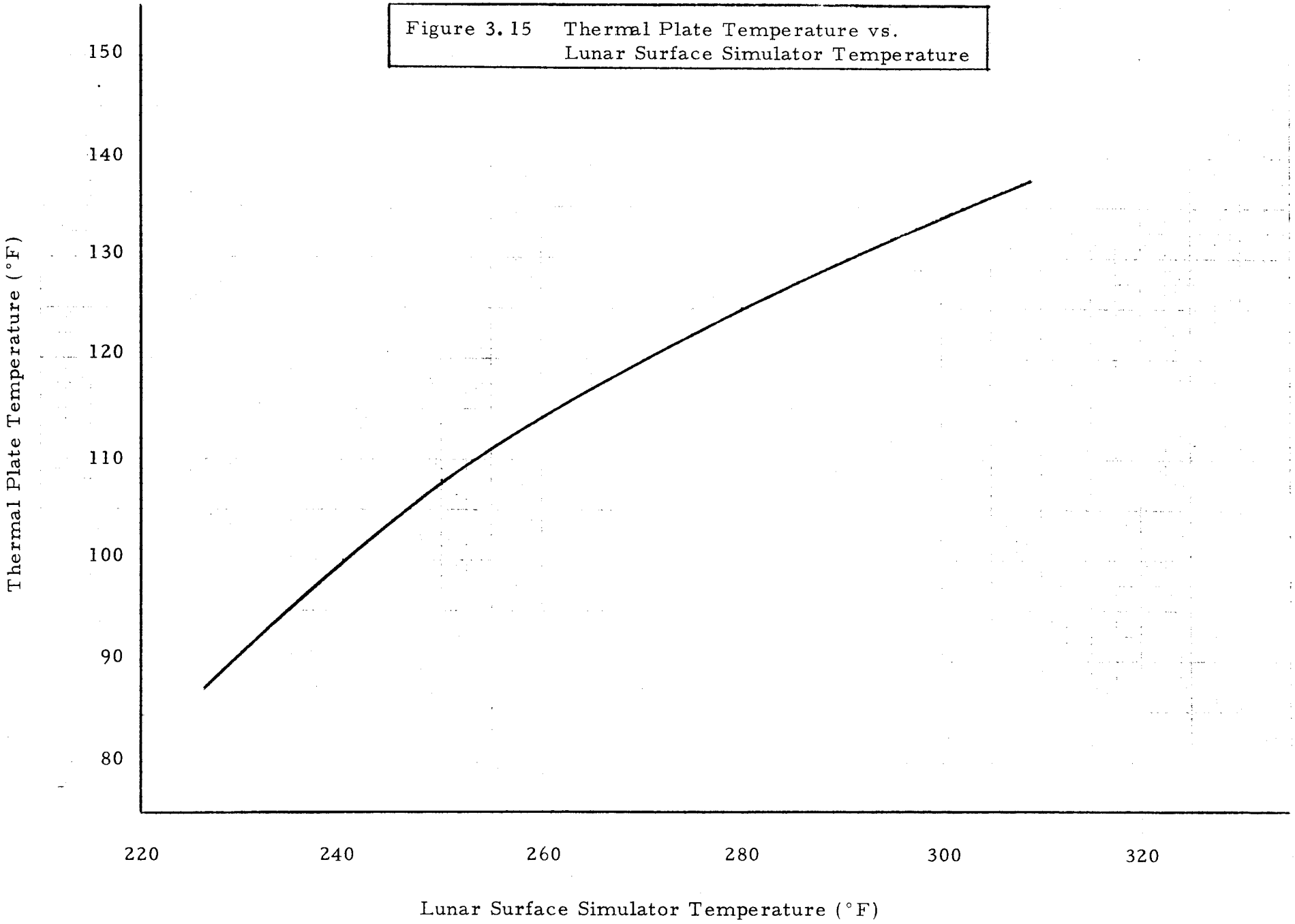

TABLE 3.6

THERMAL PLATE TEMPERATURE CORRELATION WITH TEST DATA

Test	Condition	Temperatures - °F		q_{solar} (Suns)
		Test	Analytical	
Flight 3	Noon	106.4	107.9	1.0
Flight 3	Night	39.85	45.7	0.0
QATV-SB	Noon*	132.8	133.5	1.36

*Degraded, 1.36 suns and lunar simulator temperature of 300°F.

4.0 LUNAR DEPLOYMENT

4.1 DEPLOYMENT CONSTRAINTS

The HFE has been designed to operate per the original Exhibit B specification requirement for landing sites within ±5 degrees latitude of the equator. In addition to the latitude requirement, the HFE was designed to accommodate local slopes up to a maximum of 5° at the landing sites. The worst case deployment and misalignment that can occur would be 18.5 degrees. This results from the combination of:

1. ±5 degrees variation in the landing site
2. ±12 degrees vertical misalignment
3. ±1.5 degrees for the variations of the lunar equatorial plane from the ecliptic.

4.2 Predictions for the Fra Mauro Site

Deployment is scheduled for the Fra Mauro Crater at South 4 degrees latitude. Based on this landing site and no misalignment, the

previously described analysis gives an undegraded lunar noon temperature of 100°F and a lunar night temperature of 40°F. It should be noted that the presence of heavy lunar dust coverage of the sunshield and masks would result in a considerably higher lunar noon temperature of 138°F. The above predictions are accurate to within ±5°F.

APPENDIX 1

Radiation Exchange Factors

No.	Interconnected Nodes i	j	Exchange Factor (ft^2)
1	1	101	.002177
4	2	102	.747
5	102	100	.04166
6	102	99	.04166
7	3	103	.002177
8	103	100	.01153
9	103	99	.00622
10	4	104	1.728
11	104	100	.096
12	104	99	.096
13	5	105	.002177
16	6	106	.747
17	106	100	.04166
18	106	99	.04166
19	7	107	.002177
20	107	100	.01153
21	107	99	.00622
22	8	108	1.728
23	108	100	.096
24	108	99	.096
25	9	109	2.169
26	109	100	.1205
27	109	99	.1205
28	10	110	2.169
29	110	100	.1205
30	110	99	.1205
31	11	111	3.933
33	111	99	.4925
34	12	112	3.753
37	13	113	.01806
40	14	114	.99999
43	15	115	1.5
46	16	116	1.5
47	116	100	.09844
48	116	99	.01801
49	17	117	.99999
50	117	100	.05749
51	117	99	.00438
56	102	106	.00207
57	102	112	.01984
58	102	113	.01220
59	102	118	.02896
60	103	116	.1023
61	103	117	.00896
62	103	107	.0133
63	103	117	.0329

Radiation Exchange Factors

No.	Interconnected Nodes i	j	Exchange Factor (ft^2)
70	106	113	.01220
71	106	118	.02896
72	106	112	.01220
73	107	118	.0329
74	107	116	.1023
75	107	117	.00896
79	108	121	.06888
84	110	120	.20711
85	112	118	.0295
86	112	113	.0295
89	113	118	.1198
90	116	118	.01625
91	117	118	.01525
92	22	122	.00795
93	25	125	.00795
94	26	126	.00279
95	23	123	.00279
96	24	124	.00279
97	27	127	.0033
98	28	128	.0033
99	21	121	.0279
100	19	119	.00353
101	20	120	.00353
102	122	111	.39750
133	29	129	.003373
134	30	130	.003373
135	18	118	.01806
136	118	100	.01371
317	118	99	.1926
191	1	131	.00463
192	3	133	.00463
193	5	135	.00463
194	7	137	.00463
195	131	100	.01875
196	131	99	.01875
206	101	105	.00133
207	101	113	.00329
208	101	115	.01023
209	101	114	.00896
210	105	113	.00329
211	105	114	.00896
212	105	115	.01023
213	113	114	.01525
214	113	115	.01463
215	114	115	.00572
216	101	99	.00622
217	101	100	.01153
218	105	99	.00622
219	105	100	.01153
221	113	99	.01926
222	113	100	.01371
223	114	99	.00438
224	114	100	.05749
225	115	99	.01810
226	115	100	.09844
227	112	100	.417
300	125	128	.0495
301	125	127	.0495
302	125	124	.03168
303	125	126	.03168
304	128	126	.0225
305	128	127	.0122
306	129	127	.04650
307	114	127	.05690
308	117	127	.00676
309	130	127	.0134
310	129	128	.0134
311	114	128	.00676
312	117	128	.00569
313	130	128	.0465
314	130	125	.0073
315	117	125	.00797
316	119	125	.00797
317	129	125	.0073
318	114	126	.06258
319	114	124	.06258
320	117	126	.06258
321	117	124	.06258
322	129	126	.03384
323	129	124	.03384
324	130	126	.03384
325	130	124	.03384

APPENDIX 2

Radiation Exchange Factors for Lunar Sunrise

No.	Interconnected Nodes		Exchange Factor (ft^2)		
	i	j	5°	10°	16° 45'
204	5	105	.00108	.00182	.002177
205	31	231	.00261	.00535	.00903
206	32	232	.01545	.00298	.00903
207	33	233	.00109	.00132	-
208	105	99	.00384	.00999	.00622
209		100	.00711	.00865	.01153
210	233	99	.00238	.00155	-
211	233	100	.00442	.00288	-
212	231	99	.00435	.00809	.01204
213	231	100	.0039	.00576	.00857
214	232	99	.01491	.01117	.00722
215	232	100	.00921	.0076	.00514
216	105	101	.00665	.01106	.0133
217	105	231	.000987	.0082	.0027
218	105	232	.00855	.01645	.0302
219	105	114	.0197	.05242	.0896
220	105	115	.605	.09586	.1023
221	231	101	.0047	.0109	.0302
222	231	233	.00329	.00276	-
223	231	114	.00222	.00763	.03233
224	231	115	.0206	.05182	.10306
225	232	233	.01974	.0055	-
226	232	101	.0282	.0218	.0027
227	232	114	.1503	.1409	.1202
228	232	115	.1757	.1445	.09324
229	233	101	.00665	.0022	-
230	233	114	.0699	.0372	-
231	233	115	.4018	.00694	-
232	106	231	.00174	.004	.0061
233	106	232	.01046	.0082	.0061
234	102	231	.00174	.0041	.0061
235	102	232	.01046	.0082	.0061
236	112	231	.0042	.0098	.01475
237	112	232	.0253	.0196	.01475
238	118	231	.0171	.0399	.0599
239	118	232	.1027	.0798	.0599

Note: For lunar sunrise the reflector and partially illuminated side curtain were split into two nodes representing the illuminated and non-illuminated segments. The two reflector nodes are 31 and 32. The two side curtain nodes are 5 and 33. The corresponding radiosity nodes are 231, 232, 105 and 233, respectively.

Conduction Resistances

Resistor No.	Interconnected Nodes i	j	Resistance (hr°F/Btu)
138	1	2	600.0
139	1	4	1266.
140	1	14	762.
142	2	12	4940.
143	2	13	6100.
144	2	18	6100.
145	2	2	600.
146	3	4	1266.
147	3	30	764.
148	3	17	762.5
149	4	9	1385.
150	4	10	1385.
151	4	11	405.
156	5	14	962.
157	5	29	964.5
158	5	6	600.
159	5	8	1266.
160	6	12	4940.
161	6	13	6100.
162	6	18	6100.
163	7	6	600.
164	7	17	762.
165	7	30	764.
166	7	8	1266.
167	8	9	1385.
168	8	10	1385.
169	8	11	405.
171	9	11	266.8
172	10	11	266.8
174	14	17	.128
175	14	29	.16
179	17	30	.16
180	19	28	169.
181	20	28	169.
182	21	26	199.
184	23	24	199.
190	11	99	3942.
203	22	25	4379.
204	16	30	75.
205	29	15	75.
326	29	9	91.6
327	30	10	91.6
328	29	19	71.61
329	30	20	71.61
330	29	27	91.61
331	30	28	91.61
332	19	23	2038.
333	19	21	2038.
334	20	21	2038.
335	20	23	2038.
336	27	24	1394.
337	27	26	1394.
338	28	24	1394.
339	28	26	1394.
340	25	27	986.
341	28	25	986.
342	19	22	986.
343	20	22	986.
344	14	24	1866.
345	14	26	1866.
346	14	23	4276.
347	14	21	4276.
348	17	24	1866.
349	17	26	1866.
350	17	21	4276.
351	17	21	4276.
352	14	4	570.5
353	17	4	570.5
354	14	8	570.5
355	17	8	570.5
356	24	25	1680.
357	26	25	1680.
358	23	22	2909.
359	21	22	2909.

APPENDIX 4

Changes in Enclosure Radiosity Network for Test Simulation

No.	Interconnected Nodes i	j	Exchange Factor (ft^2)
20	107	100	.00683
21	107	99	.00467
38	113	100	.01347
39	113	99	.01950
41	114	100	.05039
42	114	99	.00522
44	115	100	.09725
45	115	99	.01929
47	116	100	.09725
48	116	99	.01929
50	117	100	.05039
51	117	99	.00522
136	118	100	.01347
147	118	99	.01950

NOTE: These resistors replace the corresponding resistors in Appendix 1 for test condition simulation.

5.0 REFERENCES:

1. BxA Memo 9712-232, "Cable Heat Losses - Heat Flow Probe Electronics," 12-17-66

2. BxA Report, "Preliminary Thermal Analysis of the Heat Flow Experiment," 12-12-66

3. LMSC Report, "Thermal Analysis of the Heat Flow Experiment," 12-28-66

4. BxA Memo 9713-5-718, "HFE PDR RFC #1 and #2," 1-30-67

5. BxA Memo 9712-292, "Radiation Shield Parametric Analysis," 2-2-67

6. ADL Letter Report to Dr. M. Langseth, 2-17-67

7. Langseth, M. G. to J. Dye, "Some comments on the design of the structural housing for the Heat Flow Electronics concerning the Thermal Relation," 2-17-67

8. Gulton Industries Report, "Thermal Gradient Analysis of a Representative HFE Circuit Board and It's Heat Sink in a Vacuum," 4-17-67

9. BxA Memo 9712-393, "Heat Flow Probe Electronics - Thermal Analysis," 5-11-67

10. BxA Memo 9713-13-259, "Heat Flow Electronics Measured Power Levels, Qual 1," 11-7-67

11. BxA Memo 9713-13-414, "Boyd bolts and Guide Cups on The HFE Electronics Package," 10-4-68

12. BxA Memo 9713-10-1055, "HFE Lunar Surface Simulation - Comparison Between DVT, Proposed Proto-B and Actual Lunar Surfaces," 10-11-68

13. BxA Memo 971-482, "Removal of Boydbolts and Cups from HFE During Astronaut Deployment," 11-21-68

14. BxA Memo 68-210-132, "Guide Cup Minimum Heights," 12-6-68

15. BxA Memo 9713-12-958, "IITRI Final Report on S-13 G Adhesion to Plastic Substrates," 12-10-68

16. BxA Memo 9713-13-452, "Comparison of HFE Lunar Surface Simulation Between Eng., DVT, Qual-SB and Flight #3," 2-4-69

17. BxA Test Plan No. 9713-5-313, "HFE Electronics Box Test Plan," 1-3-77

18. BxA ATP-041, "ALSEP/Heat Flow Experiment, D-1A Thermal/Vacuum Test"

19. MSC Test Procedure SE-2102, "ALSEP HFE Thermal/ Vacuum Test," 7-10-67

20. BxA Memo 9713-13-189, "Heat Flow Experiment Design Verification Test Plan," 8-3-67

21. BxA Test Plan No. 9713-13-310, "Thermal/Vacuum Portion of HFE Electronics Box DVT Plan," 1-24-68

22. BxA Memo 70-210-16, "HFE Thermal Deployment Study," 1-20-70

23. ALSEP Technical Specification - Exhibit B, 3/10/66.

24. BxA Memo 9713-13-474, "Summary of HFE EPA Thermal Control System - BxA ALSEP Thermal/ Vacuum Tests," 5-5-69

25. IC 314109, "Interface Control Specification for Heat Flow Experiment Subsystem for Apollo Lunar Sur-Face Experiments Package," 4/10/70, Revised 5/15/69.